eLife

Neuroscience

# Microstructural asymmetries of the planum temporale predict functional lateralization of auditory-language processing

**Peipei Qin, Qiuhui Bi, Zeya Guo, Liyuan Yang, HaoKun Li, Peng Li, Xinyu Liang, Junhao Luo, Xiangyu Kong, Yirong Xiong, Bo Sun, Sebastian Ocklenburg, Gaolang Gong**

Beijing Normal University, Beijing, China • Medical School Hamburg, Hamburg, Germany



A newer version is available. **Read the latest version**.

**Version of Record**
December 16, 2024

**Reviewed Preprint**
**v2** • November 27, 2024
Revised by authors

**Reviewed Preprint**
**v1** • July 10, 2024

**eLife Assessment**

The authors studied the relationship between structural and functional lateralization in the planum temporale region of the brain, whilst also considering the morphological presentation of a single or duplicated Heschl's gyrus. The analyses are **compelling** due to a large sample size, inter-rater reliability, and corrections for multiple comparisons. The associations in this **important** work might serve as a reference for future targeted-studies on brain lateralization.

https://doi.org/10.7554/eLife.95547.2.sa2

## Abstract

Structural hemispheric asymmetry has long been assumed to guide functional lateralization of the human brain, but empirical evidence for this compelling hypothesis remains scarce. Recently, it has been suggested that microstructural asymmetries may be more relevant to functional lateralization than macrostructural asymmetries. To investigate the link between microstructure and function, we analyzed multimodal MRI data in 907 right-handed participants. We quantified structural asymmetry and functional lateralization of the planum temporale (PT), a cortical area crucial for auditory-language processing. We found associations between PT functional lateralization and several structural asymmetries, such as surface area, intracortical myelin content, neurite density, and neurite orientation dispersion. The PT structure also showed hemispheric-specific coupling with its functional activity. All these functional-structural associations are highly specific to within-PT functional activity during auditory-language processing. These results suggest that structural asymmetry underlies functional lateralization of the same brain area and highlight a critical role of microstructural PT asymmetries in auditory-language processing.

## Introduction

One compelling notion regarding brain asymmetry is that "functional lateralization is guided by structural asymmetry", hypothesizing a critical role of structural asymmetries in the neuroanatomical basis of functional lateralization (Ocklenburg and Güntürkün, 2018; Wada, 2009). As a well-known cortical area posterior to the Heschl's gyrus (HG), which includes most of the primary auditory cortex, the planum temporale (PT) putatively plays an essential role in the functional lateralization of language processing (Albouy et al., 2020; Galaburda et al., 1978; Hickok and Poeppel, 2007, 2000; Moffat et al., 1998; Price, 2010; Steinmetz, 1996; Tzourio-Mazoyer et al., 2018), and its lateralization in functional activation during auditory- or language-related tasks has been well demonstrated (Albouy et al., 2020; Hunter et al., 2003; Pahs et al., 2013; Shapleske et al., 1999; Zatorre et al., 2002). Additionally, the PT shows distinct leftward asymmetries in a variety of structural aspects, e.g., length, gray matter concentration/volume, surface area, cortical thickness, and columnar neuronal units, although the results might conflict between studies (Anderson et al., 1999; Bloom et al., 2013; Chance et al., 2008; Dorsaint-Pierre et al., 2006; Eckert et al., 2006; Fukutomi et al., 2018; Galuske et al., 2000; Greve et al., 2013; Josse et al., 2003; Knaus et al., 2006; Moffat et al., 1998; Ocklenburg et al., 2018; Schmitz et al., 2019; Sigalovsky et al., 2006; Tzourio-Mazoyer et al., 2019). Due to the role of the PT in language processing, the idea that these asymmetries may be related to leftward functional lateralization in speech processing is highly intuitive. Unexpectedly, examining the functional association of PT macrostructural asymmetries at the individual level almost always showed negative results, except for only a couple of studies demonstrating correlations between PT asymmetry of surface area and some non-PT-related indices of language lateralization, e.g., the lateralization of dichotic listening (Guadalupe et al., 2022; Hugdahl et al., 2003; Sequeira et al., 2006).

Several factors possibly account for such an unexpected majority of negative results. First, the sample size in previous studies is too small for such association analyses across individuals, compared to the recently suggested thousands of individuals for capturing a reproducible brain-wide association (Marek et al., 2022). Next, structural asymmetries were confined to PT macrostructural measures that are biologically nonspecific, e.g., surface area and thickness. Recent studies have used novel MRI techniques to quantify PT microstructure on the level of axons or dendrites and further revealed PT asymmetries in myelin content, neurite density, and neurite orientation dispersion (Fukutomi et al., 2018; Ocklenburg et al., 2018; Schmitz et al., 2019; Sigalovsky et al., 2006). Importantly, postmortem work on the microstructure of the temporal cortex has led to the hypothesis that asymmetries in the organization of the intrinsic microcircuitry of the PT and other areas may be crucial for functional lateralization (Galuske et al., 2000). In line with this idea, asymmetries in PT microstructure have been linked to electrophysiological correlates of auditory speech, an indirect measure of functional language lateralization (Ocklenburg et al., 2018). However, the crucial experiment would be to show a direct link between PT microstructure and PT functional lateralization measured with fMRI. Finally, duplicated HG (dHG) in the left or right hemisphere occurs substantially in healthy individuals, although less frequently than single HG (sHG) (Campain and Minckler, 1976; Leonard et al., 1998; Marie et al., 2015). In particular, such an HG gyrification pattern is accompanied by significant differences in PT structural properties and their asymmetries compared with the single HG (Tzourio-Mazoyer and Mazoyer, 2017). The HG gyrification pattern could further relate to the functional-structural association of PT asymmetries, therefore confounding interindividual correlation between PT asymmetries. Thus, the interindividual variation in the HG gyrification pattern should be taken into account when investigating functional-structural association of PT asymmetries, but this has been largely overlooked in previous studies.

In the present study, we included a large cohort of 907 right-handed healthy young adults to assess whether and how PT lateralization of speech-related functional activation relate to its underlying structural asymmetries. Particularly, we chose to manually delineate bilateral PTs on the virtually reconstructed cortical surface for each individual, which is very labor intensive but can localize such an anatomically highly variable structure with minimized errors. Moreover, a variety of macrostructural and microstructural measures were applied to quantify PT structural asymmetries, including surface area, cortical thickness, myelin content, neurite density index (NDI), and orientation dispersion index (ODI). Here, cortical myelin content mainly reflects the degree of intracortical axonal myelination and was measured using a noninvasive T1w/T2w mapping approach (Glasser et al., 2016; Glasser and Van Essen, 2011). Cortical NDI and ODI mainly represent the density of intracortical neurite and the complexity of dendritic arborization, respectively (Ocklenburg et al., 2018), and were estimated using the diffusion MRIbased neurite orientation dispersion and density imaging (NODDI) model (Zhang et al., 2012). Using these data, we evaluated 1) the functional and structural PT asymmetries at the group level, 2) the functional-structural coupling of PT asymmetries at the individual level, and 3) the within-hemispheric functional-structural coupling of PT at the individual level and its asymmetry. In these analyses, the influence of the HG gyrification pattern was considered.

# Results

Two experienced raters manually delineated PT and determined the HG gyrification pattern for 907 healthy right-handed young adults (**Fig 1**), with each rater assessing about half of the subjects.

As shown in **Table 1**, the manual operation showed excellent interrater reliability and imaging test-retest reproducibility for all PT measures. Among these young adults, left and right HG duplications were identified in 229 and 263 subjects, respectively (occurrence rate: left, 25.3%, right, 29.0%). In terms of the HG gyrification pattern in both hemispheres, all subjects were divided into 4 groups: 503 individuals with bilateral sHGs (L1/R1, 55.5%), 175 individuals with left sHG but right dHG (L1/R2, 19.3%), 141 individuals with left dHG but right sHG (L2/R1, 15.6%), and 88 individuals with bilateral dHGs (L2/R2, 9.7%). Age and sex did not differ among these 4 groups (**Table 2**).

The differences in age and sex distribution across the 4 groups were evaluated using one-way ANOVA and the Kruskal-Wallis test respectively. HG, Heschl's gyrus. L1/R1, single HG on the left and single HG on the right; L1/R2, single HG on the left and duplicated HG on the right; L2/R1, duplicated HG on the left and single HG on the right; L2/R2, duplicated HG on the left and duplicated HG on the right. F, female; M, male.

For each subject, fMRI activation of the left and right PT during an auditory-language comprehension task was estimated. Both left and right PTs showed significant group-level activation for all three contrasts (i.e., "story – baseline", "math – baseline", and "story – math") within the task (**Fig S1**), indicating a strong functional involvement of both PTs in such auditory-language processing. Factor analysis of the activation T values of the three contrasts revealed two factors in each hemisphere: one representing PT functional activation of speech perception and the other representing PT functional activation of speech comprehension.

We evaluated the correlation of functional and structural measures of the left and right PT with two available behavioral language test scores (the oral reading recognition test, measuring the ability of reading decoding; the picture vocabulary test, measuring the ability of linguistic comprehension), but found no significant results (all $P_{FWE} > 0.05$).

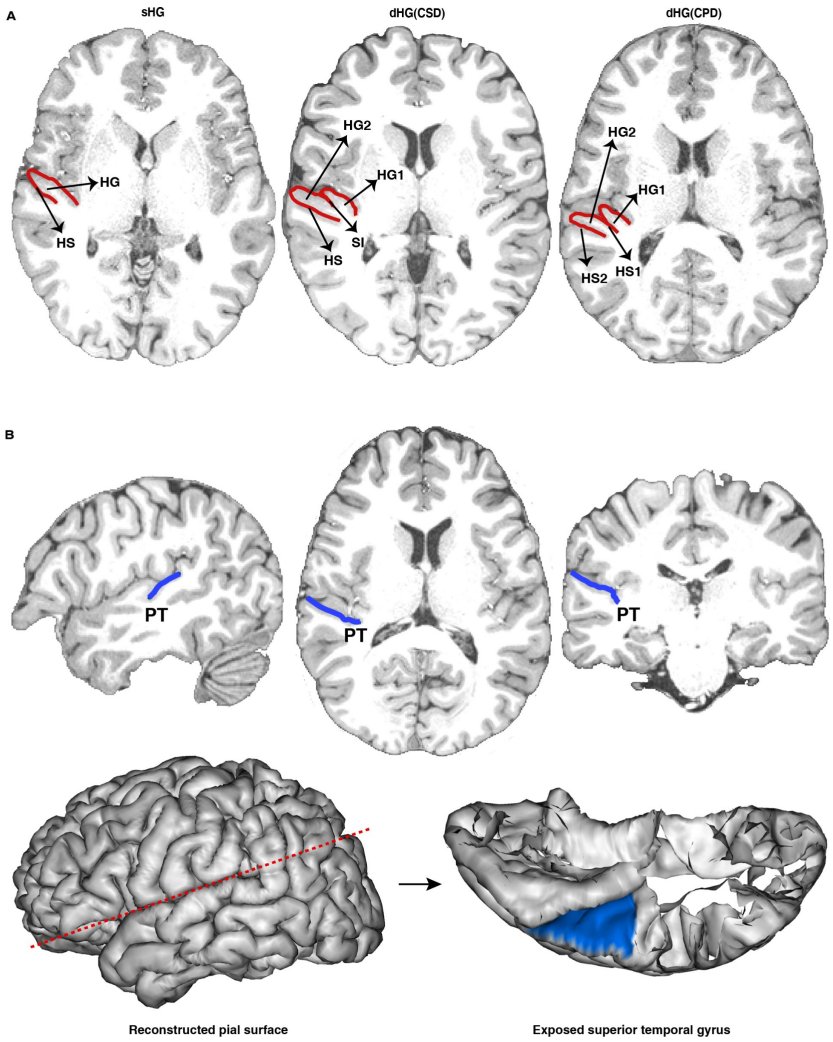


## Figure 1

### The gyrification pattern of Heschl's gyrus (HG) and manual delineation of the planum temporale (PT) on individual images.

**(A)**Examples of three types of HG gyrif cation patterns (red line): single HG (sHG), common stem duplication (CSD), and complete duplication (CPD). HG1, the anterior part of duplicated HG; HG2, the posterior part of duplicated HG; SI, the sulcus intermedius; HS1, the anterior Heschl's sulcus; HS2, the posterior Heschl's sulcus. **(B)** An example of manually delineated PT on a Tl-weighted image (blue line) and reconstructed 32k~ pial surface (blue area). The oblique section plane (red dotted line) was applied to expose the internal surface of the superior temporal gyrus using the Anatomist (Rivière et al., 2011 ).

**Table 1.**

**The reliability of PT measures from manually delineated PT**

| Reliability | | Interrater ICC (N = 20) | Imaging test-retest ICC (N = 43) |
|---|---|---|---|
| PT functional activation | Speech perception | 0.99 | 0.55 |
| | Speech comprehension | 0.99 | 0.78 |
| PT structural measures | Surface area | 0.85 | 0.69 |
| | Thickness | 0.97 | 0.72 |
| | Myelin content | 0.98 | 0.61 |
| | NDI | 0.99 | 0.73 |
| | ODI | 0.96 | 0.86 |

**Table 2.**

**The distribution of HG gyrification patterns**

| Type of HG gyrification pattern | | | | | |
|---|---|---|---|---|---|
| | L1/R1 | L1/R2 | L2/R1 | L2/R2 | Group Difference |
| Subject number | 503 | 175 | 141 | 88 | |
| Age (mean ± SD) | 28.8 ± 3.7 | 28.8 ± 3.8 | 29.2 ± 3.6 | 28.1 ± 3.6 | $p = 0.19$ |
| Sex (F/M) | 275/228 | 96/79 | 83/58 | 55/33 | $p = 0.49$ |

## PT functional and structural asymmetries at the group level

For each of the 4 groups above, PT functional lateralization of speech perception and comprehension activation were evaluated while controlling for age, gender, and brain size. As shown in **Fig 2**, significant leftward PT lateralization were observed for both speech perception and comprehension in the L1/R1(Cohen's d: speech perception = 0.35, speech comprehension = 0.36) and L1/R2 (Cohen's d: speech perception = 0.52, speech comprehension = 0.57) groups but not in the L2/R1 and L2/R2 groups (**Table S1**), suggesting a specific influence of the HG gyrification pattern on speech-related functional lateralization of the PT. For each hemisphere, we further compared these PT activations between subjects with sHG and dHG. The results showed that HG duplication was largely accompanied by decreased functional activation in the ipsilateral PT, and the degree of such a decrease varied between the left and right PTs (**Fig S2**).

Similar analyses were applied to PT structural measures, i.e., surface area, thickness, myelin content, NDI, and ODI. As shown in **Fig 3**, ODI and cortical thickness showed consistent leftward and rightward asymmetry across all 4 groups, suggesting a minimal influence of the HG gyrification pattern on the group-level PT asymmetry of these particular measures. In contrast, there was more or less confounding influence of the HG gyrification pattern on the PT asymmetry of the other 4 structural measures. Specifically, we observed 1) significant leftward asymmetry of PT surface area in the L1/R1, L1/R2, and L2/R2 groups (Cohen's d: L1/R1 = 0.42, L1/R2 = 1.48, L2/R2 = 0.73) but no asymmetry in the L2/R1 group; 2) significant leftward and rightward asymmetry of PT myelin content only in the L1/R2 and L2/R1 groups (Cohen's d: L1/R2 = 0.58, L2/R1 = -0.68); and 3) significant leftward NDI asymmetry in the L1/R2 group (Cohen's d: L1/R2 = 0.40) but rightward NDI asymmetry in both the L1/R1 and L2/R1 groups (Cohen's d: L1/R1 = -0.21, L2/R1 = -0.48) (**Table S1**). In addition, the comparison of these PT structural measures between subjects with sHG and dHG indicated that HG duplication was accompanied by a decrease in surface area, myelin content, NDI, and ODI of the ipsilateral PT, with the left and right PT also showing variable degrees of such a decrease (**Fig S3**).

We also evaluated whether functional and structural PT asymmetries correlate with the two behavioral language test scores. The AI of PT speech comprehension activation was found significantly correlated with picture vocabulary test score ($R$ = 0.10, $P_{FWE}$ = 0.047). No any other correlation was observed.

## Structure-function associations of PT asymmetries at the individual level

For each functional or structural PT measure, an asymmetry index (AI) was calculated for each subject. For each functional-structural pair of PT measures (2*5 pairs in total), we evaluated the interindividual correlation of their AIs with consideration of the HG gyrification pattern (including a group factor, i.e., L1/R1, L1/R2, L2/R1, or L2/R2), while controlling for age, gender, and brain size. No significant group effect (i.e., the interaction with the HG gyrification pattern in the general linear model) was observed for any functional-structural AI pair.

As shown in **Fig 4**, among these functional-structural pairs, the functional AI of speech perception activation showed significant positive correlations with the AIs of myelin content ($R$ = 0.26, $P_{FWE} = 1.22\times10^{-13}$), NDI ($R$ = 0.13, $P_{FWE} = 2.00\times10^{-3}$), and ODI ($R$ = 0.22, $P_{FWE} = 1.75\times10^{-9}$), regardless of the HG gyrification pattern. In contrast, functional AI of speech comprehension activation significantly correlated with the AIs of surface area ($R$ = 0.21, $P_{FWE} = 2.66\times10^{-9}$), myelin content ($R$ = 0.20, $P_{FWE} = 4.66\times10^{-8}$), and NDI ($R$ = 0.11, $P_{FWE} = 1.47\times10^{-2}$), regardless of the HG gyrification pattern. Notably, the observed interindividual correlations were consistently positive, strongly supporting an individual-level coupling of PT functional and structural asymmetries.

## Figure 2

### PT functional lateralization of speech processing at the group level.

For each group, a linear mixed model (LME) was used to test the hemispheric asymmetry of each PT functional activation. “Hemisphere” was the fixed effect, asymmetry index was the response variable, age, sex, and total brain volume were covariates. L1/R1, single HG on the left and single HG on the right; L1/R2, single HG on the left and duplicated HG on the right; L2/R1, duplicated HG on the left and single HG on the right; L2/R2, duplicated HG on the left and duplicated HG on the right. * denotes a significant difference between left and right PTs (i.e., $P_{FWE} < 0.05$). Positive and negative values of the asymmetry index represent leftward and rightward asymmetry, respectively.

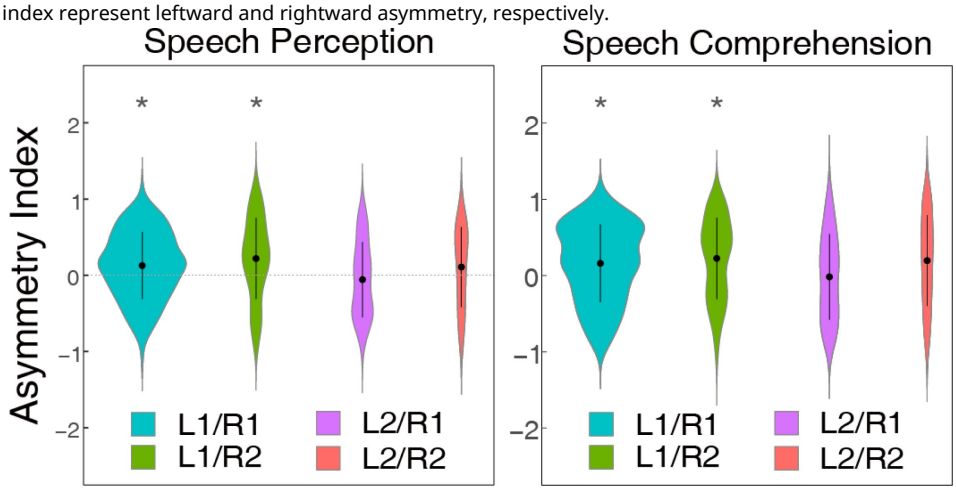


## Figure 3

### PT structural asymmetry at the group level.

For each group, a linear mixed model (LME) was used to test the hemispheric asymmetry of each PT structural measure. “Hemisphere” was the fixed effect, and asymmetry index was the response variable. Age, sex, and total brain volume were covariates. Notably, we did not standardize these structural measures, so the scales differed between indicators. L1/R1, single HG on the left and single HG on the right; L1/R2, single HG on the left and duplicated HG on the right; L2/R1, duplicated HG on the left and single HG on the right; L2/R2, duplicated HG on the left and duplicated HG on the right. NDI, neurite density index; ODI, orientation dispersion index. * denotes a significant difference between left and right PTs ($P_{FWE} < 0.05$). Positive and negative values of the asymmetry index represent leftward and rightward asymmetry, respectively.

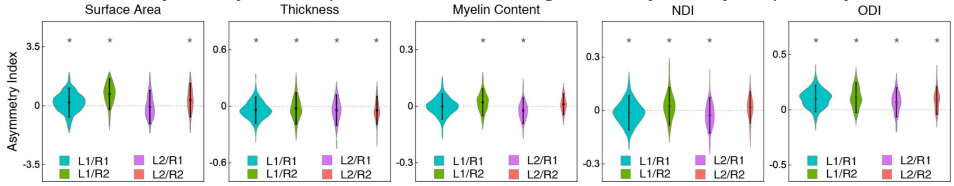

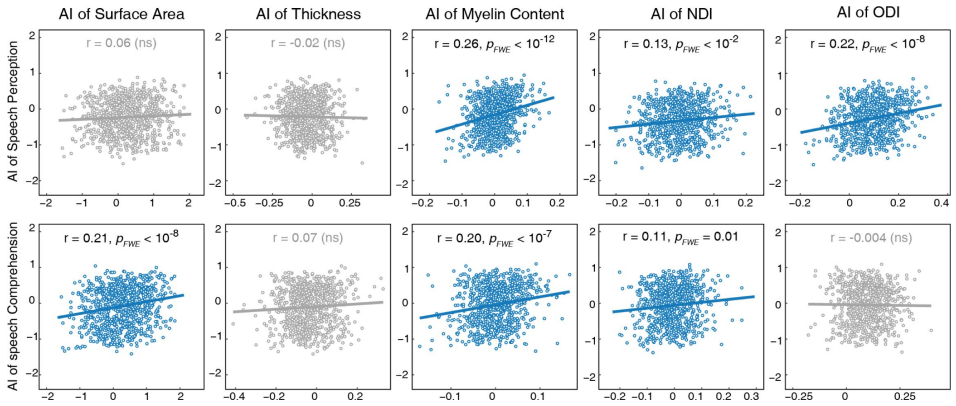


## Figure 4

### Interindividual correlation of PT functional and structural asymmetries.

For each pair of correlation, a general linear model (GLM) was used. “Functional AI” was the response variable and “structural AI”, “group”, and “structural AI × group” were predictor variables. Age, sex, and total brain volume were covariates. The scatter plots for nonsignificant correlations ($P_{FWE} > 0.05$) are colored gray. AI, asymmetry index; NDI, neurite density index; ODI, orientation dispersion index; ns, non-significant.

### Within-hemispheric PT structure-function associations at the individual level

In addition to PT functional and structural AIs, we evaluated the correlations between PT functional and structural measures of each hemisphere separately, while controlling for age, gender, and brain size (**Fig 5**). For speech perception, functional activation correlated positively with myelin content and ODI for either the left (myelin content: $R$ = 0.16, $P_{FWE}$ = 6.47×10$^{-5}$; ODI: $R$ = 0.1$^{-7}$, $P_{FWE}$ = 2.88×10$^{-5}$) or right PT (myelin content: $R$ = 0.20, $P_{FWE}$ = 1.30×10$^{-7}$; ODI: $R$ = 0.18, $P_{FWE}$ = 7.18×10$^{-6}$), regardless of the HG gyrification pattern. The permutation test, however, showed no significant difference in the degree of functional-structural correlations between the left and right PTs. Moreover, speech perception activation showed significant correlations with surface area ($R$ = -0.11, $P_{FWE}$ = 2.33×10$^{-2}$) and NDI ($R$ = 0.14, $P_{FWE}$ = 2.16×10$^{-3}$) for the right PT but not the left PT. Regarding speech comprehension, functional activation significantly correlated with myelin content for the right PT ($R$ = 0.16, $P_{FWE}$ = 2.59×10$^{-5}$) but not the left PT. We also observed a significant correlation between functional activation of speech comprehension and NDI for the left PT ($R$ = -0.12, $P_{FWE}$ = 1.62×10$^{-2}$) but not the right PT.

### Specificity of the observed PT structure-function associations

For the included subjects, another 6 task-based fMRI scans were acquired. To test whether the observed PT functional-structural couplings above are specific to auditory-language processing, we further estimated left and right PT activation of the main contrast from each of these tasks as well as their AI of PT activation, and then repeated all PT coupling analyses for these tasks. As shown in **Table S2**–**S5**, there were only very few significant correlations among the PT functional-structural pairs, therefore supporting the specificity of our currently observed PT functional-structural couplings to the functional activation of auditory-language processing.

In addition, to evaluate the spatial specificity of our observed PT functional-structural couplings, we estimated the functional activation of speech perception and comprehension of the entire hemisphere from the main auditory-language processing task. The coupling analysis showed no significant interindividual correlation between PT structural AIs and speech-related functional AIs of the entire hemisphere or between PT structural measures and speech-related functional activation of the entire ipsilateral hemisphere (**Table S6**–**S9**). Therefore, PT structural measures or their asymmetries were coupled with PT-specific functional activation or their lateralization rather than with general functional activation or its lateralization in auditory-language processing.

## Discussion

Using a large cohort of healthy adults with high-quality multimodal MRI data and highly accurate PT determination, the present study shows clear associations between structural and functional asymmetries in the PT. The observed functional-structural associations of PT asymmetries are highly specific to the within-PT functional activation of auditory-language processing.

As one of the most prominent structural asymmetries across the entire human brain, PT structural asymmetries have been well recognized and widely believed to play a critical role in human auditory or language processing (Bloom et al., 2013; Eckert and Leonard, 2000; Keller et al., 2019; Ocklenburg et al., 2018; Steinmetz, 1996; Yuan et al., 2021; Zatorre et al., 2002). The anatomical leftward asymmetry of PT emerges at an early stage of life, prior to any environmental influences such as language exposure (Dubois et al., 2010; Witelson and Pallie, 1973). This provides evidence of an early functional lateralization in the speech processing

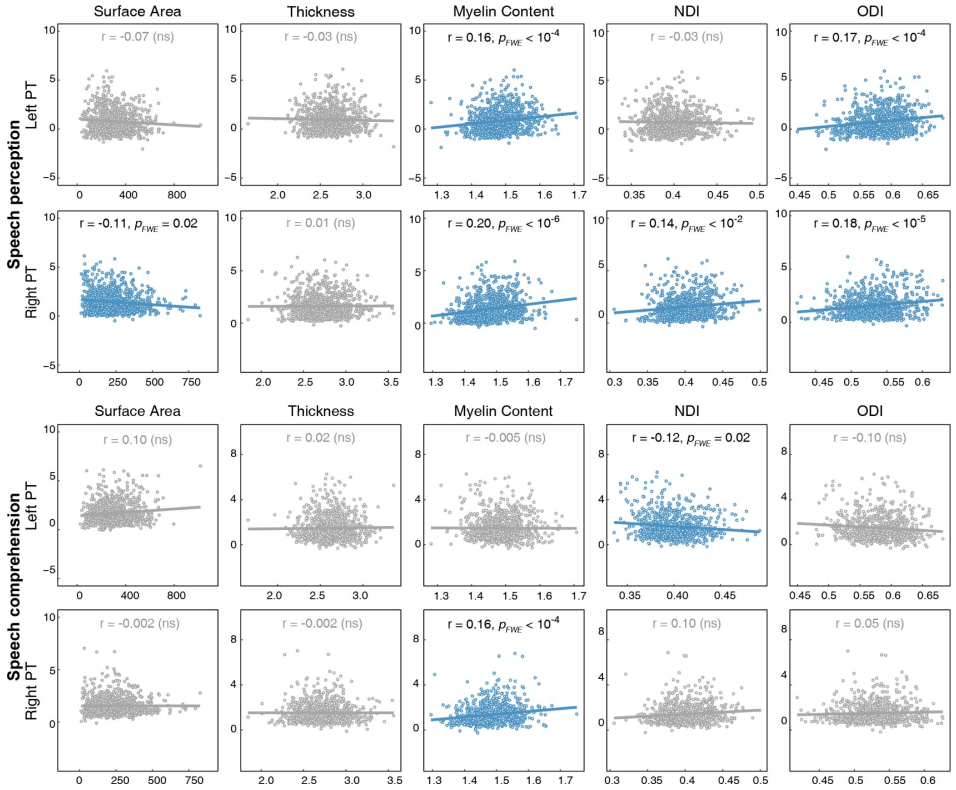


## Figure 5

### Interindividual functional-structural correlations of the left and right PT.

For each pair of correlation, a general linear model (GLM) was used. “Functional measure” was the response variable and “structural measure”, “group”, and “structural measure × group” were predictor variables. Age, sex, and hemispheric brain volume were covariates. The scatter plots for nonsignificant correlations ($P_{FWE} > 0.05$) are colored gray. NDI, neurite density index; ODI, orientation dispersion index; ns, non-significant.

capacities of the two hemispheres (Dehaene-Lambertz et al., 2002). In concordance, anomalies of PT asymmetries in surface area or thickness have been reported in various brain disorders with auditory or language deficits, e.g., dyslexia, autism, and schizophrenia (Altarelli et al., 2014; Bloom et al., 2013; Floris et al., 2016; Hynd and Semrudclikeman, 1989; Knaus et al., 2018; Pahs et al., 2013; Sumich et al., 2005, 2002; Vanderauwera et al., 2018), suggesting that asymmetric PT anatomy was an optimal architecture for the setting up of efficient speech networks. Moreover, there exist evolutionary evidence supporting the role of the PT as an anatomical substrate for language lateralization. For example, the leftward structural asymmetry of the PT have been observed in multiple non-human primates, including chimpanzees, macaques, and baboons (Becker et al., 2024; Gannon et al., 1998; Xia et al., 2019). Particularly, recent studies on baboons further demonstrated that PT structural leftward asymmetry in newborn baboons could predict future development of communicative gestures, implying a key role of PT structural asymmetry in the lateralized communication system for human and non-human brain evolution (Becker et al., 2024, 2021).

To understand the role of PT structural asymmetries in language, it is critical to determine how they relate to functional patterns of language-related processing, e.g., language-related functional lateralization. Some evidence has demonstrated an association of PT structural asymmetry with language-related functional lateralization, but these functional lateralization were not measured directly from the PT (Greve et al., 2013; Josse et al., 2003; Seghier et al., 2010; Tzourio-Mazoyer et al., 2018). For instance, PT asymmetry in surface area was correlated with regional lateralization of language-related functional activation around the Sylvian fissure but not the activation of the PT (Tzourio-Mazoyer et al., 2018). Our present study provides the first empirical evidence of interindividual associations between functional and structural asymmetries within the PT, implying a functional pathway from PT structural asymmetry to PT functional lateralization to effective speech processing. A large sample size and accurate PT localization based on well-trained manual operation were crucial in obtaining these results. Our present manually delineating method should be able to measure the PT more reliably and accurately, compared with previous atlas-based methods (Chai et al., 2021; Kuiper et al., 2020; Ocklenburg et al., 2018). The previously observed negative results of structural-functional correlation for PT asymmetries might partly attribute to coarse locating of PT regions (Greve et al., 2013; Liem et al., 2014; Tzourio-Mazoyer et al., 2018). For PT-related studies with large sample sizes, however, it is difficult to apply such a labor-intensive manual PT labeling approach, and therefore, an accurate automatic labeling approach need to be developed. Notably, our observed PT functional-structural associations were across healthy right-handed young adults, and it is unclear whether these associations could be extrapolated to children, left-handed adults, or patients. Therefore, future studies are required to evaluate the functional-structural association of PT asymmetries in other populations, which should provide insight into the modulating factor of functional-structural associations of PT.

In the context of brain asymmetries, our currently observed functional-structural coupling of PT asymmetries at the individual level empirically proves the role of structural gray matter asymmetries in the functional laterization of the same brain area, supporting the compelling hypothesis that “functional lateralization is guided by structural asymmetry” (Wada, 2009). For a specific brain area, however, its gray matter asymmetries are unlikely to be the only determinant for its functional lateralization. The relevant corpus callosum (interhemispheric connection) and structural white matter asymmetries should also play important roles in its functional lateralization, and integrating the three factors is encouraged for detangling structural mechanisms underlying functional lateralization (Allendorfer et al., 2016; Catani et al., 2007, 2005; Ocklenburg et al., 2013; Ocklenburg and Güntürkün, 2018).

The observed functional-structural coupling of PT asymmetries strongly depends on functional and structural measures. On the functional side, only PT functional activation of auditory speech processing showed such coupling with PT structural asymmetries, indicating the functional and

spatial specificity of PT lateralization in auditory-language processing (Forseth et al., 2020; Gernsbacher and Kaschak, 2003; Hickok and Poeppel, 2000; Steinmetz, 1996). Speech perception and comprehension also showed functional-structural coupling with different structural measures, compatible with the dissociation of these two speech-processing components (Dehaene-Lambertz et al., 2005; Price, 2010). It is possible that hemispheric lateralization of different functional processing are generally related to distinct structural mechanisms. However, it should be noted that the fMRI language task used in the present study was not specifically designed to study PT activation and its lateralization (Binder et al., 2011), and therefore the observed functional lateralization of speech perception and speech comprehension in the PT was not measured directly by a specific language task. Functional lateralization estimated indirectly by a data-driven approach are less specific in nature, which may partly account for the modest effect size of our observed functional-structural correlations. This also makes it difficult to further interpret the functional-structural correlation's differential pattern observed between speech perception and speech comprehension. Similarly, our specificity analyses were not based on another specifically designed language tasks for PT-associated non-speech auditory processing (e.g., reading or word production) but available task-fMRI data from the HCP. Future investigations with more specifically designed fMRI tasks on PT activation are warranted to verify and extend the PT functional-structural coupling results. On the structural side, the observed functional-structural coupling of PT asymmetries mainly involves microstructural measures, e.g., myelin content, neurite density, and neurite orientation dispersion, except for the association of speech comprehension with surface area. These microstructural measures represent specific aspects of cortical composition on the level of axons or dendrites (Glasser and Van Essen, 2011; Zhang et al., 2012), therefore implying a dominant role of within-PT microconnectional or microcircuitry asymmetries in functional asymmetries of PT. Specific microstructural asymmetry between bilateral PTs might cause less recruitment of the nondominant hemisphere in particular speech processing, therefore resulting in more pronounced functional lateralization (Galaburda et al., 1990; Tzourio-Mazoyer et al., 2018). Another possible explanation could be that higher myelin content and larger surface area in left PT potentially indicated more white matter connection with other language-related regions such as Broca's area, and therefore is more involved in language tasks than its right homolog (Allendorfer et al., 2016; Catani et al., 2005; Giampiccolo and Duffau, 2022).

Compatibly with the functional-structural coupling of PT asymmetries, most microstructural measures, including myelin content, neurite density, and neurite orientation dispersion, showed an association with speech-related activation for the left or right PT *per se*. Similar functional-structural associations have been observed in other non-PT cortical areas, e.g., between myelin content and task-evoked activities (Glasser et al., 2014; Grydeland et al., 2016; Helbling et al., 2015; Hunt et al., 2016; Kim and Knoesche, 2016; Ma and Zhang, 2017). These findings together indicate an important contribution of intracortical microcircuits to functional activity: cortical areas with greater intracortical fiber density and more complex dendritic structures are likely accompanied by stronger local activation during the task(Hall et al., 2003; Hunt et al., 2016). As for macrostructural measures, the asymmetric PT surface area was also associated with speech comprehension AI. Given that the within-hemispheric coupling tendency between surface and speech comprehension existed only in the left PT, it was possible that the larger surface area of the left PT led to a less recruitment of its right homologous, and therefore the lateralization of functional activity would be more pronounced. Additionally, an opposite tendency was found between the correlation of speech perception and comprehension with surface area, potentially implying the segregation of the different speech processing in the PT area. Intriguingly, within-hemispheric PT functional-structural coupling could be asymmetric, e.g., existing only in one hemisphere but not in the other. For instance, EEG-measured neurophysiological processing of speech perception correlated with neurite density of the left PT but not the right PT, as recently revealed by Ocklenburg and colleagues (Ocklenburg et al., 2018). Consistent with this, within-hemispheric PT functional-structural coupling of neurite density was also asymmetric in our study, highlighting the distinct role of PT neurite density in speech processing between the two

hemispheres. The distinct roles of left and right PT in speech processing have been well-documented. A number of studies substantiated that PT of the left hemisphere responded more strongly to lexical-semantic and syntactic aspects of sentence processing, whereas the right hemisphere demonstrated a greater involvement in the speech melody (Albouy et al., 2020; Meyer et al., 2002). These findings are consistent with those reported for the arcuate fasciculus (AF). The left AF has been identified as a crucial structure for language function (Giampiccolo and Duffau, 2022; Zhang et al., 2021). Disruption to this pathway has been linked to multimodal phonological and semantic deficits (Agosta et al., 2010), while injuries in the right AF did not affect language function (Zeineh et al., 2015).

The functional-structural coupling of PT asymmetries may be simply driven by the asymmetry of within-hemispheric functional-structural coupling between the left or right PT *per se*, but this is not the case. The coupling of PT asymmetries could be accompanied by either asymmetric (e.g., speech perception vs. neurite density) or nonasymmetric within-hemispheric functional-structural couplings (e.g., speech perception vs. myelin content or neurite orientation dispersion). On the other hand, asymmetric within-hemispheric structure-function association does not necessarily lead to a coupling of PT asymmetries (e.g., speech perception activation vs. surface area). Finally, PT functional and structural asymmetries could be associated, even though there was no within-hemispheric functional-structural coupling for both left and right PTs (e.g., speech comprehension activation vs. surface area). This implied that PT functional and structural asymmetries and their coupling might represent unique structural and functional information, independent of within-hemispheric PT measures. Overall, there was no simple causal relationship between these functional-structural couplings, and they likely capture distinct aspects of PT functional-structural associations and therefore should be investigated separately.

In line with previous observations (Tzourio-Mazoyer et al., 2019; Tzourio-Mazoyer and Mazoyer, 2017), HG duplication occurred considerably in healthy adults. Regardless of the HG gyrification pattern, both PT functional and structural AI showed a unimodal frequency distribution (Guadalupe et al., 2022; Packheiser et al., 2020). This contrasts with the well-documented bimodal frequency distribution of functional lateralization for speech production (Bruckert et al., 2021; Knecht et al., 2000), suggesting that the populational frequency distribution of language lateralization depends on a specific language processing module. Intriguingly, the occurrence of a left HG duplication was accompanied with a lack of the typically observed leftward asymmetry of PT activation, independent of the right HG duplication, which is consistent with previous studies (Tzourio-Mazoyer et al., 2018, 2015). This highlights a nontrivial role of the left HG duplication on functional reorganization of auditory language processing between bilateral PTs. In contrast, the HG duplication changes the PT structural asymmetries in a very complex manner, strongly depending on specific structural measure. Therefore, the impact of HG duplication on PT functional lateralization cannot be simply attributed to its impact on PT structural asymmetries. While the influence of the HG duplication on PT asymmetries has been well observed, they are largely overlooked in specific investigations, possible accounting for the result discrepancy between previous studies on PT asymmetries. Notably, no matter considering the HG duplication or not, how the asymmetries of the Heschl's gyrus and planum temporale are related remain largely unknown, and specific investigation on this topic is needed in future studies. On the other hand, the functional-structural coupling of both PT asymmetries and within-hemispheric PT measures were not significantly affected by the HG gyrification pattern. Therefore, HG duplication-induced individual changes in PT measures or their asymmetry do not necessarily lead to changes in the interindividual association between these measures or asymmetries, suggesting the robustness of these PT functional-structural couplings.

In conclusion, the association between specific PT functional and microstructural asymmetries provides direct empirical support for the contribution of structural asymmetry to functional lateralization of the same cortical area. Moreover, the findings highlight a critical role of microstructural PT asymmetries in auditory-language processing.

# Materials and methods

## Participants

In the present study, all participants of the human connectome project (HCP young adult, S1200 release) were included. The project was reviewed and approved by the Institutional Ethics Committee of Washington University in St. Louis, Missouri. The HCP young adult cohort consists of healthy individuals without neurodevelopmental, neuropsychiatric, or neurologic disorders. All participants signed written informed consent forms. For more details, please refer to Van Essen et al. (Van Essen et al., 2012).

Due to quality issues (quality control codes A and B from the HCP minimal preprocessing pipeline), 72 subjects were excluded. To control for the potential confounding effect of handedness, we included only qualified right-handed subjects (907 in total, Edinburgh Handedness questionnaire > 20) in the analysis.

## Behavioral language test

Two behavioral language tests in the NIH toolbox were applied to HCP individuals: oral reading recognition test (ORRT, measuring the ability of reading decoding) and picture vocabulary test (PVT, measuring the ability of linguistic comprehension). Given the well-documented role of PT in language processing as well as the previously reported association of PT with language performance (Blau et al., 2010; Liem et al., 2014; Tzourio-Mazoyer and Mazoyer, 2017), whether and how PT measures and their asymmetries correlate with these two language test scores were evaluated. Specifically, the age-adjusted scores for these two language tests were used in the current study.

## MRI acquisition and preprocessing

MRI data of all subjects were collected using the same 3T Siemens Skyra magnetic resonance machine at Washington University in St. Louis with a 32-channel head coil (Van Essen et al., 2012). Briefly, T1- weighted images were acquired by using a magnetized rapid gradient-echo imaging (MPRAGE) sequence with the following parameters: repetition time (TR) = 2400 ms, echo time (TE) = 2.14 ms, reversal time (TI) = 1000 ms, flip angle (FA) = 8°, field of view (FOV) = 224 × 224 $mm^2$, voxel size 0.7 mm isotropic. T2-weighted images were acquired using the variable flip angle turbo spin-echo (SPACE) sequence with the following parameters: TR = 3200 ms, TE = 565 ms, field of view (FOV) = 224 × 224 $mm^2$, voxel size 0.7 mm isotropic.

Diffusion-weighted images were acquired with spin-echo EPI with the following parameters: TR = 5520 ms, TE = 89.5 ms, field of view (FOV) = 210 × 180 $mm^2$, voxel size 1.25 mm isotropic, 111 slices, 90 directions for each of three shells of b-values (b = 1000, 2000 and 3000 $s/mm^2$) and 18 nondiffusion-weighted (b = 0 $s/mm^2$) volumes.

Task-fMRI scans were acquired under 7 tasks: language processing, working memory, incentive processing, relational processing, motor, social cognition, and emotional processing. The language processing task consisted of two runs containing 4 blocks of an auditory story task and 4 length-match blocks of an auditory math task. Specifically, during the story blocks, participants were presented with auditory stories adapted from Aesop's fables, followed by a 2-alternative forced-choice question about the topic of the story. During the math blocks, participants were presented with auditory arithmetic operations, followed by "equals" and then two choices. Participants are asked to push a button to select either the first or the second answer. For more detailed paradigms of all these tasks, please refer to Barch et al., 2013 (Barch et al., 2013). All fMRI data were

acquired by using a gradient-echo echo planar imaging (GE-EPI) sequence with the following parameters: TR = 720 ms, TE = 33.1 ms, FA = 2°, FOV = 208 × 180 $mm^2$, voxel size 2 mm isotropic, 72 slices, multiband accelerated factor = 8.

All MRI images were preprocessed using the HCP minimal preprocessing pipeline (Glasser et al., 2013). For each subject, the HCP minimal preprocessing pipeline provides the native pial and white surfaces that are resampled onto the standard 32k_fs_LR mesh (~32k vertices for each hemispheric surface).

## Manually delineating PT and determining the HG gyrification pattern

We followed a well-established procedure for manually delineating PT and determining HG gyrification patterns (Altarelli et al., 2014; Vanderauwera et al., 2018). The procedure was carried out using the Anatomist software platform embedded in BrainVISA, a sophisticated visualization and labeling tool (Geffroy et al., 2011). The Anatomist software platform allows for simultaneously localizing a given coordinate on the surface as well as on the coronal, axial, and sagittal views of the T1 image.

Two well-trained raters (Q.P. and Z.G.) blinded to the subjects' demographics carefully examined the native T1 image for each subject and determined the HG gyrification pattern according to the widely used criterion (Abdul-Kareem and Sluming, 2008). As illustrated in **Fig 1**, there were three types of HG gyrification patterns. The first is the single HG (sHG), i.e., only one transverse gyrus on the superior temporal gyrus (STG). The second is common stem duplication (CSD): the sulcus intermedius of Beck (SI) splits the HG by at least half of the length but never extends to the internal border of the gyrus. The last is complete posterior duplication (CPD): the HG is medially split into two separate parts by an additional Heschl's sulcus (HS1). In the present study, both CSD and CPD were classified as duplicated HG (dHG).

Next, the two raters performed the PT delineation on the native pial surface for each subject while simultaneously viewing the coronal, axial, and sagittal slices of the T1 image. According to Altarelli et al., 2014 (Altarelli et al., 2014), the anterior border of the PT was indicated by Heschl's sulcus or the second Heschl's sulcus; the posterior border of the PT was indicated by a change in the slope of the continuous plane characterizing the planum on the coronal view; and the lateral border was defined as the most lateral margin of the STG. For more details, please refer to Altarelli et al., 2014 and Vanderauwera et al., 2018 (Altarelli et al., 2014; Vanderauwera et al., 2018).

## PT functional activation and asymmetry index

The HCP minimal preprocessing pipeline provides individual-level *T*activation maps on the 32k_fs_LR cortical surface for three contrasts between task conditions ("story – baseline", "math – baseline", and "story – math"). For each contrast, we applied the widely-used LI-toolbox approach to quantify PT functional activation and its asymmetry index (AI). This approach avoids the dependency on a single threshold for identifying activation and proves robust and specific for computing the AI of functional activation (Wilke and Lidzba, 2007; Wilke and Schmithorst, 2006). Briefly, a number of thresholds from 0 to the maximum $T$ value of bilateral PTs were applied to the activation map of the left and right region of interest (i.e., PT). At each threshold, the $activation_{left}$, $activation_{right}$, and AI values (i.e., "$activation_{left}$ – $activation_{right}$/$activation_{left}$ + $activation_{right}$") are first estimated iteratively using a bootstrap algorithm, in which the $activation_{left}$ or $activation_{right}$ is defined as "(the total vertex area weighted $T$ values across vertices survived the threshold) / (the total number of vertices across the entire region of interest)", a measure taking into account both the relative regional size of activated vertices and their $T$ values. A histogram analysis is then followed to determine the final values for the

activation$_{left}$, activation$_{right}$, and AI. Lastly, all estimated final activation$_{left}$, activation$_{right}$ and AI values across different thresholds were weighted by their threshold, yielding the overall activation of each PTandAI values for each subject.

For either activation of each PT or AI values, there are significant correlations across individuals among the three contrasts: "story - baseline" vs. "math – baseline" (Left: $R$ = 0.93, $P_{FWE}$ < 0.001; Right: $R$ = 0.94, $P_{FWE}$ < 0.001; AI: $R$ = 0.93, $P_{FWE}$ < 0.001), "story – baseline" vs. "story – math" (Left: $R$ = 0.52, $P_{FWE}$ < 0.001; Right: $R$ = 0.47, $P_{FWE}$ < 0.001; AI: $R$ = 0.47, $P_{FWE}$ < 0.001), "math – baseline" vs. "story – math" (Left: $R$ = 0.25, $P_{FWE}$ < 0.001; Right: $R$ = 0.22, $P_{FWE}$ <0.001; AI: $R$ = 0.24, $P_{FWE}$ < 0.001). We then performed exploratory factor analysis on the PT activation$_{left}$, activation$_{right}$, and AI across the three contrasts, separately. Two main factors were consistently obtained, with one loading predominantly on the contrast of "story – math" (loadings of the activation$_{left}$: "story – baseline", 0.39; "math – baseline", 0.09; "story – math", 0.99; loadings of the activation$_{right}$: "story – baseline", 0.31; "math – baseline", 0.04; "story – math", 0.98; loadings of the AI: "story – baseline", 0.34; "math – baseline", 0.09; "story – math" , 0.99), and the other loading predominantly on the contrasts of "story – baseline" and "math – baseline" (loadings of the activation$_{left}$: "story – baseline", 0.94; "math – baseline", 0.99; "story – math", 0.21; loadings of the activation$_{right}$: "story – baseline", 0.96; "math – baseline", 0.99; "story – math", 0.21; loadings of the AI: "story – baseline", 0.93; "math – baseline", 0.99; "story – math", 0.14). Given that the contrast of "story – math" was originally designed to represent semantic processing (Binder et al., 2011) , the first main factor was therefore taken as speech comprehension. The other main factor captures a shared language processing component between the "story – baseline" and "math – baseline" and should be dissociated from speech comprehension. Therefore, the second main factor was taken as speech perception, a widely recognized function of PT and a truly shared language processing component between the "story – baseline" and "math-baseline" contrasts. The two factor scores were then used in subsequent statistical analyses.

In the first specificity analysis, we also applied the same LI-toolbox approach to compute the PT activation$_{left}$, activation$_{right}$, and AI values for the main contrast under the other 6 fMRI tasks.

In the second specificity analysis, we also applied the same LI-toolbox approach to compute the activation$_{left}$, activation$_{right}$, and AI values of the entire hemisphere for each of the three contrasts under the language task. As above, two factor scores representing functional activation of speech perception and comprehension of the entire hemisphere were estimated and applied in statistical analyses.

## PT structural measures and asymmetry index

For each subject, we directly obtained cortical maps of surface area, thickness, and T1w/T2w ratiobased myelin content from the HCP minimal preprocessing pipeline. For each delineated PT, the total surface area and averaged thickness and myelin content across PT vertices were calculated. For each subject, we also calculated the NDI and ODI using a diffusion MRI-based neurite orientation dispersion and density imaging (NODDI) approach (Zhang et al., 2012). NODDI is a highly effective method for detecting key features of neurite morphology, which employs a tissue model that detects the intracellular, extracellular and cerebrospinal fluid compartments (Zhang et al., 2012). In the grey matter of the cerebral cortex, the NDI is an estimated volume fraction of the intracellular microstructural environment, with higher NDI indicating greater neurite density. The ODI is a measure of the alignment or dispersion of neurite, with higher ODI indicating more dispersed neurite and lower ODIs indicating more aligned neurite (Jespersen et al., 2012; Zhang et al., 2012). Specifically, voxelwise values for these two measures were first estimated using AMICO (Daducci et al., 2015) and then projected onto the PT vertices using the ribbon mapping method (Marcus et al., 2011). For each delineated PT, we averaged the values of the two measures across PT vertices.

For all structural measures, the AI was computed as (Left – Right) / (Left + Right).

## Interrater reliability and test-retest reproducibility

To assess interrater reliability, the two raters both determined the HG gyrification pattern and delineated the PT for the same 20 randomly selected subjects. The results of the HG gyrification pattern reached 100% consistency. Regarding the PT measures, we calculated the intraclass correlation coefficient (ICC). As shown in **Table 1**, the interrater ICC values ranged from 0.85 to 0.99, indicating excellent interrater reliability for these measures.

To evaluate the test-retest reproducibility of both manual operation and brain imaging, one rater (P.Q.) further determined the HG gyrification pattern and delineated the PT for the 43 test-retest HCP subjects who were rescanned (test-retest interval: 1–11 months). The test-retest results of the HG gyrification pattern also reached 100% consistency. As shown in **Table 1**, the imaging test-retest ICC values ranged from 0.55 to 0.86, indicating excellent test-retest reproducibility.

## Statistical analysis

In terms of the HG gyrification pattern in both hemispheres, all subjects were divided into 4 groups: bilateral sHGs (L1/R1), left sHG but right dHG (L1/R2), left dHG but right sHG (L2/R1), and bilateral dHGs (L2/R2). The differences in age and sex distribution across the 4 groups were evaluated using one-way ANOVA and the Kruskal-Wallis test respectively. For each group, we tested the hemispheric asymmetry of each PT functional activation and structural measure. A linear mixed model (LME) was used, in which "hemisphere" was a fixed effect and "individual identity" was a random effect. In the model, age, sex, and total brain volume (Williams et al., 2022) were included as covariates. To further evaluate the influence of the HG gyrification pattern on functional and structural measures of the left and right PT, we divided all subjects into two groups for each hemisphere: sHG or dHG. The PT measures of the two groups were then compared using two-sample t tests after controlling for age, sex, and hemispheric brain volume.

We then evaluated the correlations of PT functional activation, structural measures (2*14 in total), and their AIs (2*7 pairs in total) with the scores of two behavioral language tests (i.e., ORRT and PVT), wherein age, sex, HG gyrification type and hemispheric or total brain volume were covariates.

Next, to determine whether PT structural asymmetries relate to functional lateralization at the individual level, we applied a general linear model (GLM) to each pair of functional and structural AIs (2*5 pairs in total). Specifically, the model includes "functional AI" as the response variable and "structural AI", "group" (i.e., L1/R1, L1/R2, L2/R1, or L2/R2), and "structural AI × group" as predictor variables, wherein age, sex, and total brain volume were covariates. As described previously (Chen et al., 2015; Engqvist, 2005; Zhao et al., 2019), we first evaluated whether there was a significant "structural AI × group" interaction, i.e., whether the correlation between functional and structural AIs differed between the 4 groups. If not, the term "structural AI" was assessed after excluding the interaction term; if yes, post hoc GLM analysis was conducted to assess the term "structural AI" for each of the 4 groups.

To test whether the functional-structural AI correlation is related to or even simply driven by the asymmetry of within-hemispheric PT functional-structural correlation between the left and right hemispheres, we further evaluated the correlation of PT functional activation with its structural measures within each hemisphere (4*5 pairs in total) and its asymmetry between the two hemispheres. Specifically, for each hemisphere, we applied a GLM with "functional activation" as the response variable and "structural measure", "group" (i.e., sHG or dHG), and "structural measure × group" as predictor variables, wherein age, sex, and hemispheric brain volume were covariates. Again, we first evaluated whether there was a significant "structural measure × group" interaction. If not, the term "structural measure" was assessed after excluding the interaction term; if yes, a post hoc GLM analysis was conducted to assess the term "structural measure" for

each group. For each pair of functional activation and structure measures showing a significant correlation for both the left and right PT, we then applied permutation tests to determine whether the functional-structural correlations differed between bilateral PTs.

For each type of statistical analysis above, the significance level was set as $P < 0.05$ after Bonferroni correction.


## Acknowledgements

We thank Dr. Irene Altarelli for mentoring our PT manual delineation.


## Additional information

### Additional Declarations

The authors declare no competing interests.


### Funding:

This work was supported by the China Brain Initiative grant [grant numbers 2021ZD0201701]; the China Brain Initiative grant [grant numbers 2021ZD0200502]; and the National Science Foundation of China grant [grant numbers 82172016]


### Author contributions:

Conceptualization: GG

Methodology: PQ, QB

Investigation: PQ, QB, ZG, LY, HL, PL, XL, JL, XK, YX

Visualization: PQ

Supervision: GG, BS

Writing—original draft: PQ, QB, GG

Writing—review & editing: GG, PQ, QB, SO, ZG, LY, HL, PL, XL, JL, XK, YX, BS

### Competing interests:

The authors declare no competing interests.

## Data and materials availability:

The list of HCP-subject-ID with a morphological group (L1/R1, L1/R2, etc.) is available in the supplementary material 2. The datasets analysed during the current study are available at *https://www.humanconnectome.org/*. In addition, processed data and code may be requested from the authors.

# Supplementary figures and tables

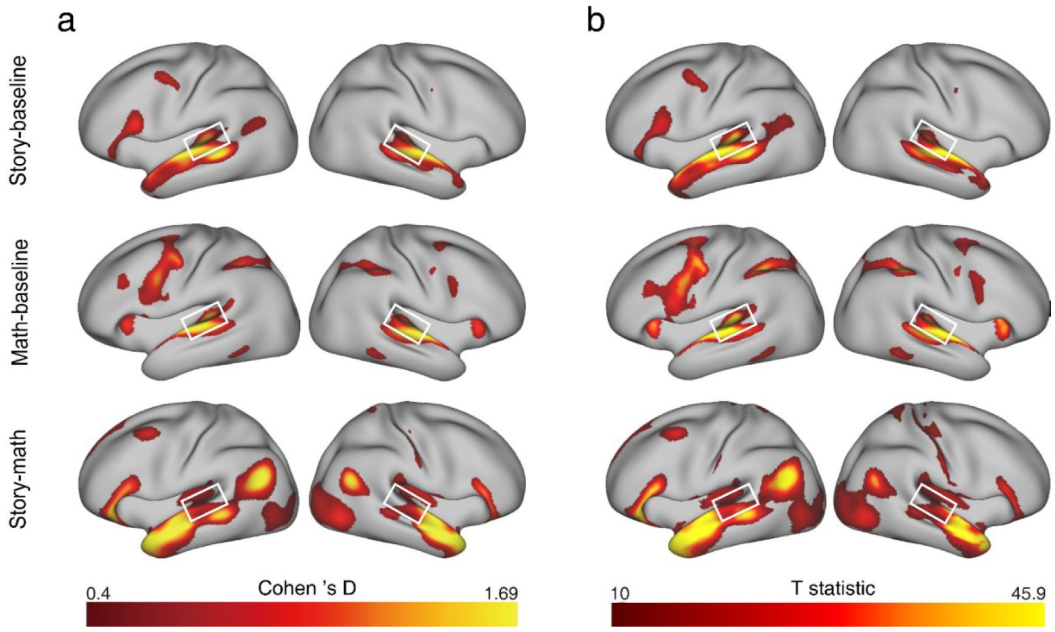


**Fig S1.**

**fMRI activation maps of the HCP language processing task.**

(a) The group Cohen's D effect size maps, showing vertices with a medium effect size (Cohen's D > 0.4). (b) Group T statistic maps from the Permutation Analysis of Linear Models (PALM), showing vertices with T>10. There were three contrasts between task conditions from this task: "story – baseline", "math – baseline", and "story – math". Statistical maps were generated from 997 subjects with quantified fMRI data. A white rectangle is placed around the PT. As shown, bilateral PTs were successfully activated under the three contrasts.

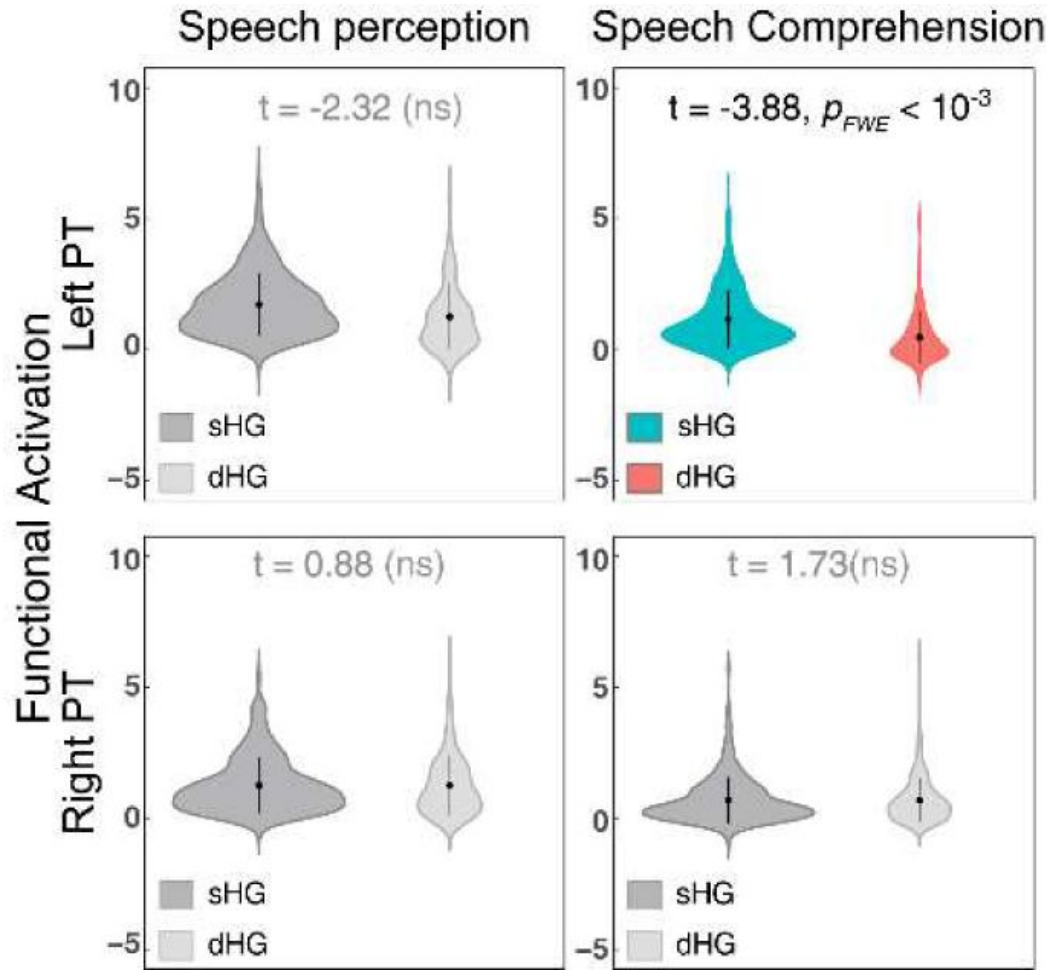


**Fig S2.**

### The difference in PT functional activation between subjects with single and duplicated HG.

The PT functional activation of the two groups were compared using two-sample t tests after controlling for age, sex, and hemispheric brain volume (ICV). sHG, single Heschl's gyrus; dHG, duplicated Heschl's gyrus; ns, non-significant. Nonsignificant differences ($P_{FWE} > 0.05$) are colored gray. Cohen's d values are listed in **Table S10**.

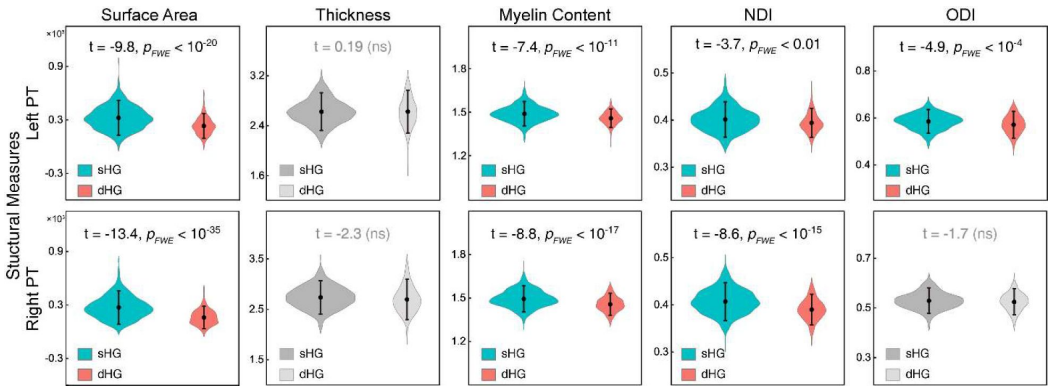

## Fig S3.

### The difference in PT structural measures between subjects with single and duplicated HG.

The PT structural measures of the two groups were compared using two-sample t tests after controlling for age, sex, and hemispheric brain volume (ICV). sHG, single Heschl's gyrus; dHG, duplicated Heschl's gyrus. Nonsignificant differences ($P_{FWE}$ > 0.05) are colored gray. NDI, neurite density index; ODI, orientation dispersion index; ns, non-significant. Cohen's d values are listed in **Table S10**

| | L1/R1 | | | L1/R2 | | | L2/R1 | | | L2/R2 | | |
|---|---|---|---|---|---|---|---|---|---|---|---|---|
| | *T* | $P_{FWE}$ | *Cohen's d* | *T* | $P_{FWE}$ | *Cohen's d* | *T* | $P_{FWE}$ | *Cohen's d* | *T* | $P_{FWE}$ | *Cohen's d* |
| **Speech perception** | **6.82** | **<.001*** | **0.35** | **5.55** | **<.001*** | **0.52** | -1.29 | >.99 | -0.10 | 1.40 | >.99 | 0.26 |
| **Speech comprehension** | **6.54** | **<.001*** | **0.36** | **6.12** | **<.001*** | **0.57** | -0.08 | >.99 | -0.12 | 2.94 | >.99 | 0.12 |
| **Surface area** | **6.83** | **<.001*** | **0.42** | **14.4** | **<.001*** | **1.48** | -2.06 | >.99 | -0.25 | **4.88** | **<.001*** | **0.73** |
| **Thickness** | **-10.0** | **<.001*** | **-0.53** | -3.08 | 0.06 | -0.30 | **-4.39** | **<.001*** | **-0.44** | -3.58 | 0.01 | -0.49 |
| **Myelin content** | -0.99 | >.99 | -0.05 | **5.97** | **<.001*** | **0.58** | **-6.50** | **<.001*** | **-0.68** | 2.67 | 0.23 | 0.36 |
| **NDI** | **-4.43** | **<.001*** | **-0.21** | **4.26** | **<.001*** | **0.40** | **-4.83** | **<.001*** | **-0.48** | 2.59 | 0.29 | 0.30 |
| **ODI** | **26.7** | **<.001*** | **1.65** | **15.8** | **<.001*** | **1.71** | **8.69** | **<.001*** | **1.03** | **9.17** | **<.001*** | **1.49** |

## Table S1.

### Group-level hemispheric asymmetry of PT functional and structural measures

| | Working memory | | Incentive processing | | Emotion processing | | Social cognition | | Motor | | Relational processing | |
|---|---|---|---|---|---|---|---|---|---|---|---|---|
| | *F* | $P_{FWE}$ | *F* | $P_{FWE}$ | *F* | $P_{FWE}$ | *F* | $P_{FWE}$ | *F* | $P_{FWE}$ | *F* | $P_{FWE}$ |
| **Surface area** | 6.54 | 0.32 | 0.68 | >.99 | 3.94 | >.99 | 0.13 | >.99 | 0.20 | >.99 | 0.04 | >.99 |
| **Thickness** | 2.06 | >.99 | 0.00 | >.99 | 0.45 | >.99 | 1.06 | >.99 | 0.80 | >.99 | 0.20 | >.99 |
| **Myelin content** | 0.03 | >.99 | 2.86 | >.99 | 0.69 | >.99 | 0.01 | >.99 | 0.19 | >.99 | 0.53 | >.99 |
| **NDI** | 1.33 | >.99 | 0.84 | >.99 | 0.01 | >.99 | 0.28 | >.99 | 0.03 | >.99 | 0.19 | >.99 |
| **ODI** | 0.32 | >.99 | 0.05 | >.99 | 0.02 | >.99 | 2.24 | >.99 | 0.35 | >.99 | 3.71 | >.99 |

## Table S2.

### The interaction effect of "PT structural AI × HG gyrification pattern" on PT nonspeech-related functional AIs (the first specificity analysis)

| | Working memory | | Incentive processing | | Emotion processing | | Social cognition | | Motor | | Relational processing | |
|---|---|---|---|---|---|---|---|---|---|---|---|---|
| | *R* | $P_{FWE}$ | *R* | $P_{FWE}$ | *R* | $P_{FWE}$ | *R* | $P_{FWE}$ | *R* | $P_{FWE}$ | *R* | $P_{FWE}$ |
| **Surface area** | **0.18** | **<.001*** | 0.09 | 0.25 | **0.21** | **<.001*** | 0.05 | >.99 | **0.18** | **<.001*** | **0.14** | **<.01*** |
| **Thickness** | 0.03 | >.99 | 0.04 | >.99 | 0.09 | 0.17 | -0.01 | >.99 | -0.08 | 0.55 | -0.01 | >.99 |
| **Myelin content** | 0.01 | >.99 | 0.02 | >.99 | 0.06 | >.99 | 0.04 | >.99 | **-0.11** | **0.04*** | -0.06 | >.99 |
| **NDI** | 0.08 | 0.64 | -0.02 | >.99 | 0.09 | 0.26 | 0.01 | >.99 | -0.08 | 0.79 | -0.06 | >.99 |
| **ODI** | -0.03 | >.99 | 0.02 | >.99 | -0.02 | >.99 | 0.08 | 0.71 | -0.08 | 0.66 | 0.00 | >.99 |

**Table S3.**

**The correlations of PT structural AIs with PT nonspeech-related functional activation AIs after controlling for the HG gyrification pattern (the first specificity analysis)**

| | | Working memory | | Incentive processing | | Emotion processing | | Social cognition | | Motor | | Relational processing | |
|---|---|---|---|---|---|---|---|---|---|---|---|---|---|
| | | *F* | $P_{FWE}$ | *F* | $P_{FWE}$ | *F* | $P_{FWE}$ | *F* | $P_{FWE}$ | *F* | $P_{FWE}$ | *F* | $P_{FWE}$ |
| **Left** | **Surface area** | 0.31 | >.99 | 0.81 | >.99 | 4.96 | >.99 | 1.93 | >.99 | 6.30 | 0.74 | 0.00 | >.99 |
| | **Thickness** | 0.17 | >.99 | 0.93 | >.99 | 0.20 | >.99 | 0.56 | >.99 | 4.59 | >.99 | 1.04 | >.99 |
| | **Myelin content** | 2.03 | >.99 | 2.24 | >.99 | 0.00 | >.99 | 7.06 | 0.48 | 4.23 | >.99 | 0.34 | >.99 |
| | **NDI** | 0.79 | >.99 | 0.59 | >.99 | 0.11 | >.99 | 6.02 | 0.86 | 0.02 | >.99 | 0.18 | >.99 |
| | **ODI** | 1.27 | >.99 | 0.01 | >.99 | 0.00 | >.99 | 0.15 | >.99 | 4.06 | >.99 | 0.31 | >.99 |
| **Right** | **Surface area** | 0.03 | >.99 | 0.03 | >.99 | 0.31 | >.99 | 0.24 | >.99 | 5.97 | 0.89 | 0.03 | >.99 |
| | **Thickness** | 0.73 | >.99 | 1.13 | >.99 | 0.90 | >.99 | 0.03 | >.99 | 1.83 | >.99 | 5.24 | >.99 |
| | **Myelin content** | 0.72 | >.99 | 1.14 | >.99 | 4.44 | >.99 | 1.10 | >.99 | **11.93** | **0.03*** | 1.68 | >.99 |
| | **NDI** | 0.06 | >.99 | 0.12 | >.99 | 1.37 | >.99 | 4.59 | >.99 | 2.86 | >.99 | 1.03 | >.99 |
| | **ODI** | 0.02 | >.99 | 1.87 | >.99 | 2.53 | >.99 | 2.00 | >.99 | 4.21 | >.99 | 0.18 | >.99 |

**Table S4.**

**The interaction effect of "PT structural measure × HG gyrification pattern" on PT nonspeech-related functional activation for each hemisphere (the first specificity analysis)**

| | | Working memory | | Incentive processing | | Emotion processing | | Social cognition | | Motor | | Relational processing | |
|---|---|---|---|---|---|---|---|---|---|---|---|---|---|
| | | *R* | $P_{FWE}$ | *R* | $P_{FWE}$ | *R* | $P_{FWE}$ | *R* | $P_{FWE}$ | *R* | $P_{FWE}$ | *R* | $P_{FWE}$ |
| Left | Surface area | -0.02 | >.99 | -0.09 | 0.42 | 0.00 | >.99 | 0.01 | >.99 | 0.01 | >.99 | -0.02 | >.99 |
| | Thickness | -0.03 | >.99 | 0.04 | >.99 | 0.04 | >.99 | 0.04 | >.99 | 0.02 | >.99 | -0.06 | >.99 |
| | Myelin content | -0.04 | >.99 | 0.02 | >.99 | -0.03 | >.99 | 0.03 | >.99 | -0.05 | >.99 | -0.04 | >.99 |
| | NDI | 0.06 | >.99 | -0.05 | >.99 | 0.00 | >.99 | -0.03 | >.99 | -0.04 | >.99 | -0.03 | >.99 |
| | ODI | -0.03 | >.99 | -0.05 | >.99 | -0.10 | 0.42 | 0.03 | >.99 | -0.04 | >.99 | 0.02 | >.99 |
| Right | Surface area | -0.05 | >.99 | -0.03 | >.99 | -0.05 | >.99 | **-0.12** | **0.02*** | 0.06 | >.99 | -0.06 | >.99 |
| | Thickness | 0.05 | >.99 | 0.01 | >.99 | 0.08 | 0.75 | -0.05 | >.99 | -0.01 | >.99 | 0.00 | >.99 |
| | Myelin content | -0.05 | >.99 | 0.01 | >.99 | 0.02 | >.99 | -0.01 | >.99 | **-0.23** | **<.001*** | -0.09 | 0.43 |
| | NDI | 0.00 | >.99 | 0.01 | >.99 | -0.01 | >.99 | 0.00 | >.99 | **-0.14** | **<.01*** | -0.11 | 0.15 |
| | ODI | -0.02 | >.99 | 0.03 | >.99 | 0.06 | >.99 | 0.01 | >.99 | **-0.25** | **<.001*** | 0.00 | >.99 |

**Table S5.**

**The correlations of PT structural measures with PT nonspeech-related functional activation for each hemisphere after controlling for the HG gyrification pattern (the first specificity analysis)**

| | | Entire hemisphere | | | |
|---|---|---|---|---|---|
| | | Speech perception | | Speech comprehension | |
| | | *F* | $P_{FWE}$ | *F* | $P_{FWE}$ |
| PT | Surface area | 0.10 | >.99 | 0.27 | >.99 |
| | Thickness | 0.15 | >.99 | 0.02 | >.99 |
| | Myelin content | 0.10 | >.99 | 2.24 | >.99 |
| | NDI | 0.05 | >.99 | 0.59 | >.99 |
| | ODI | 0.38 | >.99 | 1.34 | >.99 |

**Table S6.**

**The interaction effect of "PT structural AI × HG gyrification pattern" on speech-related functional AIs of the entire hemisphere (the second specificity analysis)**

| | | Entire hemisphere | | | |
|---|---|---|---|---|---|
| | | Speech perception | | Speech comprehension | |
| | | *R* | $P_{FWE}$ | *R* | $P_{FWE}$ |
| PT | Surface area | -0.05 | >.99 | 0.03 | >.99 |
| | Thickness | -0.07 | 0.47 | -0.05 | >.99 |
| | Myelin content | -0.02 | >.99 | 0.06 | 0.89 |
| | NDI | -0.06 | >.99 | 0.05 | >.99 |
| | ODI | 0.02 | >.99 | 0.02 | >.99 |

**Table S7.**

**hemisphere after controlling for the HG gyrification pattern (the second specificity analysis)**

| | | Entire ipsilateral hemisphere | | | |
|---|---|---|---|---|---|
| | | Speech perception | | Speech comprehension | |
| | | $F$ | $P_{FWE}$ | $F$ | $P_{FWE}$ |
| Left PT | Surface area | 3.74 | >.99 | 0.63 | >.99 |
| | Thickness | 0.11 | >.99 | 0.86 | >.99 |
| | Myelin content | 0.31 | >.99 | 0.86 | >.99 |
| | NDI | 0.39 | >.99 | 1.25 | >.99 |
| | ODI | 0.15 | >.99 | 1.35 | >.99 |
| Right PT | Surface area | 0.44 | >.99 | 0.30 | >.99 |
| | Thickness | 0.45 | >.99 | 1.35 | >.99 |
| | Myelin content | 0.52 | >.99 | 0.10 | >.99 |
| | NDI | 0.71 | >.99 | 0.03 | >.99 |
| | ODI | 3.68 | >.99 | 0.00 | >.99 |

**Table S8.**

**The interaction effect of "PT structural measure × HG gyrification pattern" on speech-related functional activation of the entire ipsilateral hemisphere (the second specificity analysis)**

| | | Entire ipsilateral hemisphere | | | |
|---|---|---|---|---|---|
| | | Speech perception | | Speech comprehension | |
| | | $R$ | $P_{FWE}$ | $R$ | $P_{FWE}$ |
| Left PT | Surface area | 0.00 | >.99 | 0.07 | >.99 |
| | Thickness | -0.04 | >.99 | -0.07 | 0.99 |
| | Myelin content | -0.02 | >.99 | 0.03 | >.99 |
| | NDI | -0.08 | 0.62 | -0.05 | >.99 |
| | ODI | 0.02 | >.99 | 0.02 | >.99 |
| Right PT | Surface area | 0.02 | >.99 | 0.01 | >.99 |
| | Thickness | 0.03 | >.99 | 0.02 | >.99 |
| | Myelin content | 0.02 | >.99 | -0.01 | >.99 |
| | NDI | 0.04 | >.99 | -0.01 | >.99 |
| | ODI | 0.02 | >.99 | -0.02 | >.99 |

**Table S9.**

**The correlations of PT structural measures with speech-related functional activation of the entire ipsilateral hemisphere after controlling for the HG gyrification pattern (the second specificity analysis)**

| | Left hemisphere | Right hemisphere |
|---|---|---|
| Speech perception | 0.20 | 0.04 |
| Speech comprehension | **0.37** | 0.12 |
| Surface area | **0.77** | **0.98** |
| Thickness | 0.02 | 0.17 |
| Myelin content | **0.57** | **0.65** |
| NDI | **0.30** | **0.67** |
| ODI | **0.41** | 0.14 |

**Table S10.**

**The difference in PT functional and structural metrices between groups with single and duplicated HG within each hemisphere (the effect size, Cohen's D).**

# References


Abdul-Kareem IA, Sluming V (2008) **Heschl gyrus and its included primary auditory cortex: Structural MRI studies in healthy and diseased subjects** *J Magn Reson Imaging* https://doi.org/10.1002/jmri.21445

Agosta F *et al.* (2010) **Language networks in semantic dementia** *Brain J Neurol* **133**:286–299 https://doi.org/10.1093/brain/awp233

Albouy P, Benjamin L, Morillon B, Zatorre RJ (2020) **Distinct sensitivity to spectrotemporal modulation supports brain asymmetry for speech and melody** *Science* **367**:1043–1047 https://doi.org/10.1126/science.aaz3468

Allendorfer JB, Hernando KA, Hossain S, Nenert R, Holland SK, Szaflarski JP (2016) **Arcuate fasciculus asymmetry has a hand in language function but not handedness** *Hum Brain Mapp* **37**:3297–3309 https://doi.org/10.1002/hbm.23241

Altarelli I, Leroy F, Monzalvo K, Fluss J, Billard C, Dehaene-Lambertz G, Galaburda AM, Ramus F (2014) **Planum Temporale Asymmetry in Developmental Dyslexia: Revisiting an Old Question** *Hum Brain Mapp, 20191219* **35**:5717–5735 https://doi.org/10.1002/hbm.22579

Anderson B, Southern BD, Powers RE (1999) **Anatomic asymmetries of the posterior superior temporal lobes: a postmortem study** *Neuropsychiatry Neuropsychol Behav Neurol* **12**:247–254

Barch DM *et al.* (2013) **Function in the Human Connectome: Task-fMRI and Individual Differences in Behavior** *NeuroImage* **80**:169–189 https://doi.org/10.1016/j.neuroimage.2013.05.033

Becker Y *et al.* (2024) **Planum temporale asymmetry in newborn monkeys predicts the future development of gestural communication's handedness** *Nat Commun* **15** https://doi.org/10.1038/s41467-024-47277-6

Becker Y, Sein J, Velly L, Giacomino L, Renaud L, Lacoste R, Anton J-L, Nazarian B, Berne C, Meguerditchian A (2021) **Early Left-Planum Temporale Asymmetry in newborn monkeys (Papio anubis): A longitudinal structural MRI study at two stages of development** *NeuroImage* **227** https://doi.org/10.1016/j.neuroimage.2020.117575

Binder JR *et al.* (2011) **Mapping anterior temporal lobe language areas with fMRI: A multicenter normative study** *NeuroImage* **54**:1465–1475 https://doi.org/10.1016/j.neuroimage.2010.09.048

Blau V, Reithler J, van Atteveldt N, Seitz J, Gerretsen P, Goebel R, Blomert L (2010) **Deviant processing of letters and speech sounds as proximate cause of reading failure: a functional magnetic resonance imaging study of dyslexic children** *Brain* **133**:868–879 https://doi.org/10.1093/brain/awp308

Bloom JS, Garcia-Barrera MA, Miller CJ, Miller SR, Hynd GW (2013) **Planum temporale morphology in children with developmental dyslexia** *Neuropsychologia* **51**:1684–1692 https://doi.org/10.1016/j.neuropsychologia.2013.05.012

Bruckert L, Thompson PA, Watkins KE, Bishop DVM, Woodhead ZVJ (2021) **Investigating the effects of handedness on the consistency of lateralization for speech production and semantic processing tasks using functional transcranial Doppler sonography** *Laterality* **26**:680–705 https://doi.org/10.1080/1357650X.2021.1898416

Campain R, Minckler J (1976) **A note on the gross configurations of the human auditory cortex** *Brain Lang* **3**:318–323 https://doi.org/10.1016/dkjwsw

Catani M, Allin MPG, Husain M, Pugliese L, Mesulam MM, Murray RM, Jones DK (2007) **Symmetries in human brain language pathways correlate with verbal recall** *Proc Natl Acad Sci* **104**:17163–17168 https://doi.org/10.1073/pnas.0702116104

Catani M, Jones DK, Ffytche DH (2005) **Perisylvian language networks of the human brain** *Ann Neurol* **57**:8–16 https://doi.org/10.1002/ana.20319

Chai Y, Liu TT, Marrett S, Li L, Khojandi A, Handwerker DA, Alink A, Muckli L, Bandettini PA (2021) **Topographical and laminar distribution of audiovisual processing within human planum temporale** *Prog Neurobiol* **205** https://doi.org/10.1016/j.pneurobio.2021.102121

Chance SA, Casanova MF, Switala AE, Crow TJ (2008) **Auditory cortex asymmetry, altered minicolumn spacing and absence of ageing effects in schizophrenia** *Brain* **131**:3178–3192 https://doi.org/10.1093/brain/awn211

Chen Y, Li P, Gu B, Liu Z, Li X, Evans AC, Gong G, Zhang Z (2015) **The Effects of an APOE Promoter Polymorphism on Human Cortical Morphology during Nondemented Aging** *J Neurosci* **35**:1423–1431 https://doi.org/10.1523/jneurosci.1946-14.2015

Daducci A, Canales-Rodríguez EJ, Zhang H, Dyrby TB, Alexander DC, Thiran J-P (2015) **Accelerated Microstructure Imaging via Convex Optimization (AMICO) from diffusion MRI data** *NeuroImage* **105** https://doi.org/10.1016/j.neuroimage.2014.10.026

Dehaene-Lambertz G, Dehaene S, Hertz-Pannier L (2002) **Functional Neuroimaging of Speech Perception in Infants** *Science* **298**:2013–2015 https://doi.org/10.1126/science.1077066

Dehaene-Lambertz G, Pallier C, Serniclaes W, Sprenger-Charolles L, Jobert A, Dehaene S (2005) **Neural correlates of switching from auditory to speech perception** *NeuroImage* **24**:21–33 https://doi.org/10.1016/j.neuroimage.2004.09.039

Dorsaint-Pierre R, Penhune VB, Watkins KE, Neelin P, Lerch JP, Bouffard M, Zatorre RJ (2006) **Asymmetries of the planum temporale and Heschl's gyrus: relationship to language lateralization** *Brain* **129**:1164–1176 https://doi.org/10.1093/brain/awl055

Dubois J, Benders M, Lazeyras F, Borradori-Tolsa C, Leuchter RH-V, Mangin JF, Hueppi PS (2010) **Structural asymmetries of perisylvian regions in the preterm newborn** *Neuroimage* **52**:32–42 https://doi.org/10.1016/j.neuroimage.2010.03.054

Eckert MA, Leonard CM (2000) **Structural imaging in dyslexia: The planum temporale** *Ment Retard Dev Disabil Res Rev* **6**:198–206 https://doi.org/10.1002/1098-2779(2000)6:3<198::AID-MRDD7>3.0.CO;2-1

Eckert MA, Leonard CM, Possing ET, Binder JR (2006) **Uncoupled leftward asymmetries for planum morphology and functional language processing** *Brain Lang* **98**:102–111 https://doi.org/10.1016/j.bandl.2006.04.002

Engqvist L (2005) **The mistreatment of covariate interaction terms in linear model analyses of behavioural and evolutionary ecology studies** *Anim Behav* **70**:967–971 https://doi.org/10.1016/j.anbehav.2005.01.016

Floris DL *et al.* (2016) **Atypically Rightward Cerebral Asymmetry in Male Adults With Autism Stratifies Individuals With and Without Language Delay** *Hum Brain Mapp* **37**:230–253 https://doi.org/10.1002/hbm.23023

Forseth KJ, Hickok G, Rollo PS, Tandon N (2020) **Language prediction mechanisms in human auditory cortex** *Nat Commun* **11** https://doi.org/10.1038/s41467-020-19010-6

Fukutomi H, Glasser MF, Zhang H, Autio JA, Coalson TS, Okada T, Togashi K, Van Essen DC, Hayashi T (2018) **Neurite imaging reveals microstructural variations in human cerebral cortical gray matter** *Neuroimage* **182**:488–499 https://doi.org/10.1016/j.neuroimage.2018.02.017

Galaburda A, LeMay M, Kemper T, Geschwind N (1978) **Right-left asymmetrics in the brain** *Science* **199**:852–856 https://doi.org/10.1126/science.341314

Galaburda AM, Rosen GD, Sherman GF (1990) **Individual variability in cortical organization: its relationship to brain laterality and implications to function** *Neuropsychologia* **28**:529–546 https://doi.org/10.1016/0028-3932(90)90032-j

Galuske RA, Schlote W, Bratzke H, Singer W (2000) **Interhemispheric asymmetries of the modular structure in human temporal cortex** *Science* **289**:1946–1949 https://doi.org/10.1126/science.289.5486.1946

Gannon PJ, Holloway RL, Broadfield DC, Braun AR (1998) **Asymmetry of Chimpanzee Planum Temporale: Humanlike Pattern of Wernicke's Brain Language Area Homolog** *Science* **279**:220–222 https://doi.org/10.1126/science.279.5348.220

Geffroy D, Rivière D, Denghien I, Souedet N, Laguitton S, Cointepas Y (2011) **BrainVISA: a complete software platform for neuroimaging 2**

Gernsbacher MA, Kaschak MP (2003) **Neuroimaging studies of language production and comprehension** *Annu Rev Psychol* **54**:91–114 https://doi.org/10.1146/annurev.psych.54.101601.145128

Giampiccolo D, Duffau H (2022) **Controversy over the temporal cortical terminations of the left arcuate fasciculus: a reappraisal** *Brain J Neurol awac057* https://doi.org/10.1093/brain/awac057

Glasser MF *et al.* (2016) **A multi-modal parcellation of human cerebral cortex** *Nature* **536**:171–178 https://doi.org/10.1038/nature18933

Glasser MF, Goyal MS, Preuss TM, Raichle ME, Van Essen DC (2014) **Trends and Properties of Human Cerebral Cortex: Correlations with Cortical Myelin Content** *NeuroImage* **93**:165–175 https://doi.org/10.1016/j.neuroimage.2013.03.060

Glasser MF *et al.* (2013) **The minimal preprocessing pipelines for the Human Connectome Project** *NeuroImage* **80**:105–124 https://doi.org/10.1016/j.neuroimage.2013.04.127

Glasser MF, Van Essen DC (2011) **Mapping human cortical areas in vivo based on myelin content as revealed by T1- and T2-weighted MRI** *J Neurosci Off J Soc Neurosci* **31**:11597–11616 https://doi.org/10.1523/JNEUROSCI.2180-11.2011

Greve DN, Van der Haegen L, Cai Q, Stufflebeam S, Sabuncu MR, Fischl B, Brysbaert M (2013) **A Surfacebased Analysis of Language Lateralization and Cortical Asymmetry** *J Cogn Neurosci* **25**:1477–1492 https://doi.org/10.1162/jocn_a_00405

Grydeland H, Westlye LT, Walhovd KB, Fjell AM (2016) **Intracortical Posterior Cingulate Myelin Content Relates to Error Processing: Results from T1- and T2-Weighted MRI Myelin Mapping and Electrophysiology in Healthy Adults** *Cereb Cortex* **26**:2402–2410 https://doi.org/10.1093/cercor/bhv065

Guadalupe T, Kong X-Z, Akkermans SEA, Fisher SE, Francks C (2022) **Relations between hemispheric asymmetries of grey matter and auditory processing of spoken syllables in 281 healthy adults** *Brain Struct Funct* **227**:561–572 https://doi.org/10.1007/s00429-021-02220-z

Hall DA, Hart HC, Johnsrude IS (2003) **Relationships between Human Auditory Cortical Structure and Function** *Audiol Neurotol* **8**:1–18 https://doi.org/10.1159/000067894

Helbling S, Teki S, Callaghan MF, Sedley W, Mohammadi S, Griffiths TD, Weiskopf N, Barnes GR (2015) **Structure predicts function: Combining non-invasive electrophysiology with in-vivo histology** *NeuroImage* **108**:377–385 https://doi.org/10.1016/j.neuroimage.2014.12.030

Hickok G, Poeppel D (2007) **The cortical organization of speech processing** *Nat Rev Neurosci* **8** https://doi.org/10.1038/nrn2113

Hickok G, Poeppel D (2000) **Towards a functional neuroanatomy of speech perception** *Trends Cogn Sci* **4**:131–138 https://doi.org/10.1016/S1364-6613(00)01463-7

Hugdahl K, Heiervang E, Ersland L, Lundervold A, Steinmetz H, Smievoll AI (2003) **Significant relation between MR measures of planum temporale area and dichotic processing of syllables in dyslexic children** *Neuropsychologia* **41**:666–675 https://doi.org/10.1016/S0028-3932(02)00224-5

Hunt BAE, Tewarie PK, Mougin OE, Geades N, Jones DK, Singh KD, Morris PG, Gowland PA, Brookes MJ (2016) **Relationships between cortical myeloarchitecture and electrophysiological networks** *Proc Natl Acad Sci U S A* **113**:13510–13515 https://doi.org/10.1073/pnas.1608587113

Hunter MD, Griffiths TD, Farrow TFD, Zheng Y, Wilkinson ID, Hegde N, Woods W, Spence SA, Woodruff PWR (2003) **A neural basis for the perception of voices in external auditory space** *Brain* **126**:161–169 https://doi.org/10.1093/brain/awg015

Hynd GW, Semrudclikeman M (1989) **DYSLEXIA AND BRAIN MORPHOLOGY** *Psychol Bull* **106**:447–482 https://doi.org/10.1037/0033-2909.106.3.447

Jespersen SN, Leigland LA, Cornea A, Kroenke CD (2012) **Determination of Axonal and Dendritic Orientation Distributions Within the Developing Cerebral Cortex by Diffusion Tensor Imaging** *IEEE Trans Med Imaging* **31**:16–32 https://doi.org/10.1109/TMI.2011.2162099

Josse G, Mazoyer B, Crivello F, Tzourio-Mazoyer N (2003) **Left planum temporale: an anatomical marker of left hemispheric specialization for language comprehension** *Cogn Brain Res* **18**:1–14 https://doi.org/10.1016/j.cogbrainres.2003.08.007

Keller M, Neuschwander P, Meyer M (2019) **When right becomes less right: Neural dedifferentiation during suprasegmental speech processing in the aging brain** *Neuroimage* **189**:886–895 https://doi.org/10.1016/j.neuroimage.2019.01.050

Kim S-G, Knoesche TR (2016) **Intracortical myelination in musicians with absolute pitch: Quantitative morphometry using 7-T MRI** *Hum Brain Mapp* **37**:3486–3501 https://doi.org/10.1002/hbm.23254

Knaus TA, Bollich AM, Corey DM, Lemen LC, Foundas AL (2006) **Variability in perisylvian brain anatomy in healthy adults** *Brain Lang* **97**:219–232 https://doi.org/10.1016/j.bandl.2005.10.008

Knaus TA, Kamps J, Foundas AL, Tager-Flusberg H (2018) **Atypical PT anatomy in children with autism spectrum disorder with expressive language deficits** *Brain Imaging Behav* **12**:1419–1430 https://doi.org/10.1007/s11682-017-9795-7

Knecht S, Deppe M, Dräger B, Bobe L, Lohmann H, Ringelstein E, Henningsen H (2000) **Language lateralization in healthy right-handers** *Brain J Neurol* **123**:74–81 https://doi.org/10.1093/brain/123.1.74

Kuiper JJ *et al.* (2020) **A parcellation-based model of the auditory network** *Hear Res* **396** https://doi.org/10.1016/j.heares.2020.108078

Leonard CM, Puranik C, Kuldau JM, Lombardino LJ (1998) **Normal variation in the frequency and location of human auditory cortex landmarks** *Heschl's gyrus: where is it? Cereb Cortex* **8**:397–406 https://doi.org/10.1093/cercor/8.5.397

Liem F, Hurschler MA, Jäncke L, Meyer M (2014) **On the planum temporale lateralization in suprasegmental speech perception: Evidence from a study investigating behavior, structure, and function** *Hum Brain Mapp* **35**:1779–1789 https://doi.org/10.1002/hbm.22291

Ma Z, Zhang N (2017) **Cross-population myelination covariance of human cerebral cortex** *Hum Brain Mapp* **38**:4730–4743 https://doi.org/10.1002/hbm.23698

Marcus DS, Harwell J, Olsen T, Hodge M, Glasser MF, Prior F, Jenkinson M, Laumann T, Curtiss SW, Van Essen DC (2011) **Informatics and Data Mining Tools and Strategies for the Human Connectome Project** *Front Neuroinformatics* **5** https://doi.org/10.3389/fninf.2011.00004

Marek S *et al.* (2022) **Reproducible brain-wide association studies require thousands of individuals** *Nature* **603** https://doi.org/10.1038/s41586-022-04492-9

Marie D, Jobard G, Crivello F, Perchey G, Petit L, Mellet E, Joliot M, Zago L, Mazoyer B, Tzourio-Mazoyer N (2015) **Descriptive anatomy of Heschl's gyri in 430 healthy volunteers, including 198 left-handers** *Brain Struct Funct* **220**:729–743 https://doi.org/10.1007/s00429-013-0680-x

Meyer M, Alter K, Friederici AD, Lohmann G, von Cramon DY (2002) **FMRI reveals brain regions mediating slow prosodic modulations in spoken sentences** *Hum Brain Mapp* **17**:73–88 https://doi.org/10.1002/hbm.10042

Moffat SD, Hampson E, Lee DH (1998) **Morphology of the planum temporale and corpus callosum in left handers with evidence of left and right hemisphere speech representation** *Brain* **121**:2369–2379 https://doi.org/10.1093/brain/121.12.2369

Ocklenburg S, Friedrich P, Fraenz C, Schlüter C, Beste C, Güntürkün O, Genç E (2018) **Neurite architecture of the planum temporale predicts neurophysiological processing of auditory speech** *Sci Adv 4:eaar6830* https://doi.org/10.1126/sciadv.aar6830

Ocklenburg S, Güntürkün O (2018) **The lateralized brain: the neuroscience and evolution of hemispheric asymmetries** London ; San Diego, CA: Elsevier/Academic Press

Ocklenburg S, Hugdahl K, Westerhausen R (2013) **Structural white matter asymmetries in relation to functional asymmetries during speech perception and production** *NeuroImage* **83**:1088–1097 https://doi.org/10.1016/j.neuroimage.2013.07.076

Packheiser J, Schmitz J, Arning L, Beste C, Güntürkün O, Ocklenburg S (2020) **A large-scale estimate on the relationship between language and motor lateralization** *Sci Rep* **10** https://doi.org/10.1038/s41598-020-70057-3

Pahs G, Rankin P, Cross JH, Croft L, Northam GB, Liegeois F, Greenway S, Harrison S, Vargha-Khadem F, Baldeweg T (2013) **Asymmetry of planum temporale constrains interhemispheric language plasticity in children with focal epilepsy** *Brain* **136**:3163–3175 https://doi.org/10.1093/brain/awt225

Price CJ (2010) **The anatomy of language: a review of 100 fMRI studies published in 2009** *Ann N Y Acad Sci* **1191**:62–88 https://doi.org/10.1111/j.1749-6632.2010.05444.x

Rivière D, Geffroy D, Denghien I, Souedet N, Cointepas Y (2011) **Anatomist: a python framework for interactive 3D visualization of neuroimaging data 2**

Schmitz J, Fraenz C, Schlüter C, Friedrich P, Jung RE, Güntürkün O, Genç E, Ocklenburg S (2019) **Hemispheric asymmetries in cortical gray matter microstructure identified by neurite orientation dispersion and density imaging** *NeuroImage* **189**:667–675 https://doi.org/10.1016/gft49q

Seghier ML, Kherif F, Josse G, Price CJ (2010) **Regional and hemispheric determinants of language laterality: Implications for preoperative fMRI** *Hum Brain Mapp* **32**:1602–1614 https://doi.org/10.1002/hbm.21130

Sequeira SD, Woerner W, Walter C, Kreuder F, Lueken U, Westerhausen R, Wittling RA, Schweiger E, Wittling W (2006) **Handedness, dichotic-listening ear advantage, and gender effects on planum temporale asymmetry - A volumetric investigation using structural magnetic resonance imaging** *Neuropsychologia* **44**:622–636 https://doi.org/10.1016/j.neuropsychologia.2005.06.014

Shapleske J, Rossell SL, Woodruff PW, David AS (1999) **The planum temporale: a systematic, quantitative review of its structural, functional and clinical significance** *Brain Res Brain Res Rev* **29**:26–49 https://doi.org/10.1016/cz9bk7

Sigalovsky IS, Fischl B, Melcher JR (2006) **Mapping an intrinsic MR property or gray matter in auditory cortex of living humans: A possible marker for primary cortex and hemispheric differences** *Neuroimage* **32**:1524–1537 https://doi.org/10.1016/j.neuroimage.2006.05.023

Steinmetz H (1996) **Structure, function and cerebral asymmetry: In vivo morphometry of the planum temporale** *Neurosci Biobehav Rev* **20**:587–591 https://doi.org/10.1016/0149-7634(95)00071-2

Sumich A, Chitnis XA, Fannon DG, O'Ceallaigh S, Doku VC, Faldrowicz A, Sharma T (2005) **Unreality symptoms and volumetric measures of Heschl's gyrus and planum temporal in first-episode psychosis** *Biol Psychiatry* **57**:947–950 https://doi.org/10.1016/j.biopsych.2004.12.041

Sumich A, Chitnis XA, Fannon DG, O'Ceallaigh S, Doku VC, Falrowicz A, Marshall N, Matthew VM, Potter M, Sharma T (2002) **Temporal lobe abnormalities in first-episode psychosis** *Am J Psychiatry* **159** https://doi.org/10.1176/appi.ajp.159.7.1232

Tzourio-Mazoyer N, Crivello F, Mazoyer B (2018) **Is the planum temporale surface area a marker of hemispheric or regional language lateralization?** *Brain Struct Funct* **223**:1217–1228 https://doi.org/10.1007/s00429-017-1551-7

Tzourio-Mazoyer N, Maingault S, Panzieri J, Pepe A, Crivello F, Mazoyer B (2019) **Intracortical Myelination of Heschl's Gyrus and the Planum Temporale Varies With Heschl's Duplication Pattern and Rhyming Performance: An Investigation of 440 Healthy Volunteers** *Cereb Cortex* **29**:2072–2083 https://doi.org/10.1093/cercor/bhy088

Tzourio-Mazoyer N, Mazoyer B (2017) **Variations of planum temporale asymmetries with Heschl's Gyri duplications and association with cognitive abilities: MRI investigation of 428 healthy volunteers** *Brain Struct Funct* **222**:2711–2726 https://doi.org/10.1007/s00429-017-1367-5

Van Essen DC *et al.* (2012) **The Human Connectome Project: a data acquisition perspective** *NeuroImage* **62**:2222–2231 https://doi.org/10.1016/j.neuroimage.2012.02.018

Vanderauwera J, Altarelli I, Vandermosten M, De Vos A, Wouters J, Ghesquiere P (2018) **Atypical Structural Asymmetry of the Planum Temporale is Related to Family History of Dyslexia** *Cereb Cortex* **28**:63–72 https://doi.org/10.1093/cercor/bhw348

Wada JA (2009) **Is functional hemispheric lateralization guided by structural cerebral asymmetry** *Can J Neurol Sci J Can Sci Neurol* **36**:S25–31

Wilke M, Lidzba K (2007) **LI-tool: A new toolbox to assess lateralization in functional MR-data** *J Neurosci Methods* **163**:128–136 https://doi.org/10.1016/j.jneumeth.2007.01.026

Wilke M, Schmithorst VJ (2006) **A combined bootstrap/histogram analysis approach for computing a lateralization index from neuroimaging data** *NeuroImage* **33**:522–530 https://doi.org/10.1016/j.neuroimage.2006.07.010

Williams CM, Peyre H, Toro R, Ramus F (2022) **Comparing brain asymmetries independently of brain size** *NeuroImage* **254** https://doi.org/10.1016/j.neuroimage.2022.119118

Witelson SF, Pallie W (1973) **Left hemisphere specialization for language in the newborn. Neuroanatomical evidence of asymmetry** *Brain J Neurol* **96**:641–646 https://doi.org/10.1093/brain/96.3.641

Xia J, Wang F, Wu Z, Wang L, Zhang C, Shen D, Li G (2019) **Mapping hemispheric asymmetries of the macaque cerebral cortex during early brain development** *Hum Brain Mapp* https://doi.org/10.1002/hbm.24789

Yuan D, Luo D, Kwok VPY, Zhou Y, Tian H, Yu Q, An J, Gao J-H, Qiu S, Tan LH (2021) **Myeloarchitectonic Asymmetries of Language Regions in the Human Brain** *Cereb Cortex* **31**:4169–4179 https://doi.org/10.1093/cercor/bhab076

Zatorre RJ, Belin P, Penhune VB (2002) **Structure and function of auditory cortex: music and speech** *Trends Cogn Sci* **6**:37–46 https://doi.org/10.1016/S1364-6613(00)01816-7

Zeineh MM, Kang J, Atlas SW, Raman MM, Reiss AL, Norris JL, Valencia I, Montoya JG (2015) **Right arcuate fasciculus abnormality in chronic fatigue syndrome** *Radiology* **274**:517–526 https://doi.org/10.1148/radiol.14141079

Zhang H, Schneider T, Wheeler-Kingshott CA, Alexander DC (2012) **NODDI: Practical in vivo neurite orientation dispersion and density imaging of the human brain** *NeuroImage* **61**:1000–1016 https://doi.org/10.1016/j.neuroimage.2012.03.072

Zhang J *et al.* (2021) **Correlations between Dual-Pathway White Matter Alterations and Language Impairment in Patients with Aphasia: A Systematic Review and Meta-analysis** *Neuropsychol Rev* **31**:402–418 https://doi.org/10.1007/s11065-021-09482-8

Zhao C, Yang L, Xie S, Zhang Z, Pan H, Gong G (2019) **Hemispheric Module-Specific Influence of the X Chromosome on White Matter Connectivity: Evidence from Girls with Turner Syndrome** *Cereb Cortex* **29**:4580–4594 https://doi.org/10.1093/cercor/bhy335

## Author information

**Peipei Qin**
Beijing Normal University, Beijing, China

**Qiuhui Bi**
Beijing Normal University, Beijing, China

**Zeya Guo**
Beijing Normal University, Beijing, China

**Liyuan Yang**
Beijing Normal University, Beijing, China

**HaoKun Li**
Beijing Normal University, Beijing, China

**Peng Li**
Beijing Normal University, Beijing, China

**Xinyu Liang**
Beijing Normal University, Beijing, China

**Junhao Luo**
Beijing Normal University, Beijing, China

**Xiangyu Kong**
Beijing Normal University, Beijing, China

**Yirong Xiong**
Beijing Normal University, Beijing, China

**Bo Sun**
Beijing Normal University, Beijing, China

**Sebastian Ocklenburg**
Medical School Hamburg, Hamburg, Germany

**Gaolang Gong**
Beijing Normal University, Beijing, China
ORCID iD: 0000-0001-5788-022X

**For correspondence:** gao1ang.gong@bnu.edu.cn

## Editors

Reviewing Editor
**Adrien Meguerditchian**
CNRS, Aix-Marseille University, Marseille, France

Senior Editor
**Barbara Shinn-Cunningham**
Carnegie Mellon University, Pittsburgh, United States of America

**Reviewer #1 (Public review):**

Summary:

Qin and colleagues analysed data from the Human Connectome Project on four right-handed subgroups with different gyrification patterns in Heschl's gyrus. Based on these groups, the authors highlight the structure-function relationship of planum temporale asymmetry in lateralised language processing at the group level and next at the individual level. In particular, the authors propose that especially microstructural asymmetries are related to functional auditory language asymmetries in the planum temporale.

Strengths:

The study is interesting because of an ongoing and long-standing debate about the relationship between structural and functional brain asymmetries, and in particular whether structural brain asymmetries can be seen as markers of functional language brain lateralisation.

In this debate, the relationship between Heschl's gyrus asymmetry and planum temporale asymmetry is rare and therefore valuable here. A large sample size and inter-rater reliability support the findings.

Weaknesses:

The authors highlight the microstructural results, but could also emphasise on their interesting macrostructural results.

https://doi.org/10.7554/eLife.95547.2.sa1

**Author response:**

The following is the authors' response to the original reviews.

> ***Reviewer #1 (Public Review):***
>
> *Summary:*
>
> *Qin and colleagues analysed data from the Human Connectome Project on four right-handed subgroups with different gyrification patterns in Heschl's gyrus. Based on these groups, the authors highlight the structure-function relationship of planum temporale asymmetry in lateralised language processing at the group level and next at the individual level. In particular, the authors propose that especially microstructural asymmetries are related to functional auditory language asymmetries in the planum temporale.*
>
> *Strengths:*
>
> *The study is interesting because of an ongoing and long-standing debate about the relationship between structural and functional brain asymmetries, and in particular whether structural brain asymmetries can be seen as markers of functional language brain lateralisation.*
>
> *In this debate, the relationship between Heschl's gyrus asymmetry and planum temporale asymmetry is rare and therefore valuable here. A large sample size and inter-rater reliability support the findings.*
>
> *Weaknesses:*
>
> *In this case of multiple brain measures, it would be important to provide the reader with some sort of effect size (e.g. Cohen's d) to help interpret the results.*

Thank you for pointing this out. In the revised version, the effect size, i.e., Cohen's d, has been incorporated into the results (page 8, line 159-160; page 9, line 181-186, supplementary page 14, Table S14).

> *In addition, the authors highlight the microstructural results in spite of the macrostructural results. However, the macrostructural surface results are also strong. I would suggest either reducing the emphasis on micro vs macrostructural results or adding information to justify the microstructural importance.*

In the original manuscript, we highlighted the results of microstructural measures because the correlations between PT microstructural and functional measures were more pronounced both within the hemispheres and in terms of asymmetry, compared with the significant results of surface area. Following your comments here, we now lowered the tone of microstructure results (page 2, line 40; page 14, line 267), and added relevant discussion regarding the macrostructural results in the revised version (page 18, line 363-370; as copied below):

"As for macrostructural measures, the asymmetric PT surface area was also associated with speech comprehension AI. Given that the within-hemispheric coupling tendency between surface and speech comprehension existed only in the left PT, it was possible that the larger surface area of the left PT led to a less recruitment of its right homologous, and therefore the lateralization of functional activity would be more pronounced. Additionally, an opposite tendency was found between the correlation of speech perception and comprehension with

surface area, potentially implying the segregation of the different speech processing in the PT area."

> ***Recommendations for the authors:***
>
> *I have only some comments that I wish to be addressed by the authors:*
>
> *(1) Please always specify "structural" or "functional" asymmetry or lateralisation, as the reader may be confused.*

This has been done in relevant places.

> *(2) Please state that the scale is not the same between the results in Figure 3.*

This have been specified, as suggested (see below).

"Notably, we did not standardize these structural measures, so the scales differed between indicators."

> *(3) It may be of interest to the reader to learn more about interpretations of how Heschl's gyrus and planum temporale asymmetries are related.*

Thank you for this comment. Given that the asymmetry of Heschl's gyrus was not analyzed in the present study, we do not have direct data/results for such an interpretation. Also, we reviewed the literature but found no relevant results on how Heschl's gyrus and planum temporale asymmetries are related. To address this, specific investigation targeting on this topic is needed. This has now been added in the discussion (page 20, line 415-417).

> *(4) As this manuscript builds somewhat on the Science Advances article by Ocklenburg et al. (2018), it would be important to discuss how this more liberal planum temporale definition might (or might not) affect the results compared to the more conservative planum temporale definition described here.*

Yes, the definition of planum temporale varies across studies. Our current manual one is relatively more conservative than the Ocklenburg et al. (2018), in which the planum temporale was automatically derived from the Destrieux atlas. We believe that the definition of the planum temporale likely have non-trivial impact on the results, and our current manual definition with the consideration of the HG duplication should be more reliable and accurate, therefore favored, relative to the other ones. This has been briefly discussed in the revision (page 15-16, line 300-304).

> *(5) I would like the authors to briefly but critically discuss what exactly the MRI NODDI model measures and how this is interpreted as measuring microstructural properties of tissue.*

We now provided relevant information regarding the NODDI measures (page 26, line 552-558; as copied below).

"NODDI is a highly effective method for detecting key features of neurite morphology, which employs a tissue model that detects three microstructural environments: the intracellular, extracellular and cerebrospinal fluid compartments (Zhang et al., 2012). In the grey matter of the cerebral cortex, the neurite density index (NDI) is an estimated volume fraction of the intracellular microstructural environment, with higher NDIs indicating greater neurite density (Jespersen et al., 2010; Zhang et al., 2012). The orientation dispersion index (ODI) is a measure of the alignment or dispersion of neurite, with higher ODIs indicating more

dispersed neurite and lower ODIs indicating more aligned neurite (Jespersen et al., 2012; Zhang et al., 2012)."

> *(6) While not mandatory, I would be interested to read the authors' thoughts on the evolution of such a functional/(micro)structural lateralisation link of the planum temporale, in light of the literature on planum temporale asymmetries in (newborn) non-human primate species.*

Thank you for this inspiring suggestion. We have incorporated relevant discussion into the revised version (page 15, line 281-288; as copied below).

"Moreover, there exist evolutionary evidence supporting the role of the PT as an anatomical substrate for language lateralization. For example, the leftward structural asymmetry of the PT have been observed in multiple non-human primates, including chimpanzees, macaques, and baboons (Becker et al., 2024; Gannon et al., 1998; Xia et al., 2019). Particularly, recent studies on baboons further demonstrated that PT structural leftward asymmetry in newborn baboons could predict future development of communicative gestures, implying a key role of PT structural asymmetry in the lateralized communication system for human and non-human brain evolution (Becker et al., 2024, 2021)."

Reference

Becker Y, Phelipon R, Marie D, Bouziane S, Marchetti R, Sein J, Velly L, Renaud L, Cermolacce A, Anton J-L, Nazarian B, Coulon O, Meguerditchian A. 2024. Planum temporale asymmetry in newborn monkeys predicts the future development of gestural communication's handedness. *Nat Commun* 15:4791. doi:10.1038/s41467-024-47277-6

Becker Y, Sein J, Velly L, Giacomino L, Renaud L, Lacoste R, Anton J-L, Nazarian B, Berne C, Meguerditchian A. 2021. Early Left-Planum Temporale Asymmetry in newborn monkeys (Papio anubis): A longitudinal structural MRI study at two stages of development. *NeuroImage* 227:117575. doi:10.1016/j.neuroimage.2020.117575

Gannon PJ, Holloway RL, Broadfield DC, Braun AR. 1998. Asymmetry of Chimpanzee Planum Temporale: Humanlike Pattern of Wernicke's Brain Language Area Homolog. *Science* 279:220–222. doi:10.1126/science.279.5348.220

Jespersen SN, Bjarkam CR, Nyengaard JR, Chakravarty MM, Hansen B, Vosegaard T, Østergaard L, Yablonskiy D, Nielsen NChr, Vestergaard-Poulsen P. 2010. Neurite density from magnetic resonance diffusion measurements at ultrahigh field: Comparison with light microscopy and electron microscopy. *NeuroImage* 49:205–216. doi:10.1016/j.neuroimage.2009.08.053

Jespersen SN, Leigland LA, Cornea A, Kroenke CD. 2012. Determination of Axonal and Dendritic Orientation Distributions Within the Developing Cerebral Cortex by Diffusion Tensor Imaging. *IEEE Trans Med Imaging* 31:16–32. doi:10.1109/TMI.2011.2162099

Xia J, Wang F, Wu Z, Wang L, Zhang C, Shen D, Li G. 2019. Mapping hemispheric asymmetries of the macaque cerebral cortex during early brain development. *Hum Brain Mapp*. doi:10.1002/hbm.24789

Zhang H, Schneider T, Wheeler-Kingshott CA, Alexander DC. 2012. NODDI: Practical in vivo neurite orientation dispersion and density imaging of the human brain. *NeuroImage* 61:1000–1016. doi:10.1016/j.neuroimage.2012.03.072

> ***Reviewer #2 (Public Review):***
>
> *Summary:*

> *The authors assessed the link between structural and functional lateralization in area PT, one of the brain areas that is known to exhibit strong structural lateralization, and which is known to be implicated in speech processing. Importantly, they included the sulcal configuration of Heschl's gyrus (HG), presenting either as a single or duplicated HG, in their analysis. They found several significant associations between microstructural indices and task-based functional lateralization, some of which depended on the sulcal configuration.*
>
> *Strengths:*
>
> *A clear strength is the large sample size (n=907), an openly available database, and the fact that HG morphology was manually classified in each individual. This allows for robust statistical testing of the effects across morphological categories, which is not often seen in the literature.*
>
> *Weaknesses:*
>
> *- Unfortunately, no left-handers were included in the study. It would have been a valuable addition to the literature, to study the effect of handedness on the observed associations, as many previous studies on this topic were not adequately powered. The fact that only right-handers were studied should be pointed out clearly in the introduction or even the abstract.*

Thank for pointing this out. We have explicitly specified this in the Abstract and Introduction.

> *- The tasks to quantify functional lateralization were not specifically designed to pick up lateralization. In the interest of the sample size, it is understandable that the authors used the available HCP-task-battery results, however, it would have been feasible to access another dataset for validation. A targeted subset of results, concerning for example the relationship between sulcal morphology and task-based functional lateralization, could be re-assessed using other open-access fMRI datasets.*

Yes, the fMRI task was not specifically designed to evaluate PT functional lateralization, which has been acknowledged in the discussion (page 17, line 330-342). Given the observed small effect size of our current structural-functional relationship, reproducing similar results with other datasets would require a cohort with a large sample size. This would induce a quite labor-intensive work given our current manual protocol for outlining PT and HG for everyone. The lack of validation with independent dataset has been discussed as a limitation in the revised version. We will try to conduct such a validation in future work, likely after developing an automatic pipeline for accurately extracting the PT and HG in the individual space (like the manual outlining protocol).

> *- The study is mainly descriptive and the general discussion of the findings in the larger context of brain lateralization comes a bit short. For example, are the observed effects in line with what we know from other 'language-relevant' areas? What could be the putative mechanisms that give rise to functional lateralization based on the microstructural markers observed? And which mechanisms might be underlying the formation of a duplicated HG?*

Thank you for these insightful comments. As suggested, we strengthened the discussion as below:

“Another possible explanation could be that higher myelin content and larger surface area in left PT potentially indicated more white matter connection with other language-related

regions such as Broca's area, and therefore is more involved in language tasks than its right homolog (Allendorfer et al., 2016; Catani et al., 2005; Giampiccolo and Duffau, 2022).

The distinct roles of left and right PT in speech processing have been well-documented. A number of studies substantiated that PT of the left hemisphere responded more strongly to lexical-semantic and syntactic aspects of sentence processing, whereas the right hemisphere demonstrated a greater involvement in the speech melody (Albouy et al., 2020; Meyer et al., 2002).

These findings are consistent with those reported for the arcuate fasciculus (AF). The left AF has been identified as a crucial structure for language function (Giampiccolo and Duffau, 2022; Zhang et al., 2021). Disruption to this pathway has been linked to multimodal phonological and semantic deficits (Agosta et al., 2010), while injuries in the right AF did not affect language function (Zeineh et al., 2015)."

Regarding the mechanism underlying the formation of a duplicated HG, we did not come up with good thoughts after careful literature review. Also, we feel that this is kind of out of the scope of the present study and therefore did not add more discussion on this topic.

> ***Recommendations for the authors:***
>
> *(1) The data availability statement makes no explicit mention of the manual labels of HG configuration. Would the authors consider making available a list of HCP-subject-ID with a morphological group (L1/R1, L1/R2, etc.) for replicability and for re-use by other researchers?*

The list of HCP-subject-ID with a morphological group (L1/R1, L1/R2, etc.) is now available in the supplementary material 2. We have specified this in the revised version.

> *(2) It would be helpful to state again the statistical tests associated with the p-value in the figure/table caption, e.g. Table 2.*

As suggested, we now specified the statistical method in the figure/table caption.

> *(3) Sometimes, the y-axis labels are missing or not clear, for example in Figure S2.*

Sorry about these. We double-checked all the figures, and corrected the missing or unclear labels for Figure S2 and S3 in the revised version.

> *(4) In a few instances the font sizes vary within a figure caption.*

This has been corrected in the revision.

Reference

Agosta F, Henry RG, Migliaccio R, Neuhaus J, Miller BL, Dronkers NF, Brambati SM, Filippi M, Ogar JM, Wilson SM, Gorno-Tempini ML. 2010. Language networks in semantic dementia. *Brain J Neurol* **133**:286–299. doi:10.1093/brain/awp233

Albouy P, Benjamin L, Morillon B, Zatorre RJ. 2020. Distinct sensitivity to spectrotemporal modulation supports brain asymmetry for speech and melody. *Science* **367**:1043–1047. doi:10.1126/science.aaz3468

Allendorfer JB, Hernando KA, Hossain S, Nenert R, Holland SK, Szaflarski JP. 2016. Arcuate fasciculus asymmetry has a hand in language function but not handedness. *Hum Brain Mapp* **37**:3297–3309. doi:10.1002/hbm.23241

Catani M, Jones DK, Ffytche DH. 2005. Perisylvian language networks of the human brain. *Ann Neurol* **57**:8–16. doi:10.1002/ana.20319

Giampiccolo D, Duffau H. 2022. Controversy over the temporal cortical terminations of the left arcuate fasciculus: a reappraisal. *Brain J Neurol* **145**:1242–1256. doi:10.1093/brain/awac057

Meyer M, Alter K, Friederici AD, Lohmann G, von Cramon DY. 2002. FMRI reveals brain regions mediating slow prosodic modulations in spoken sentences. *Hum Brain Mapp* **17**:73–88. doi:10.1002/hbm.10042

Zeineh MM, Kang J, Atlas SW, Raman MM, Reiss AL, Norris JL, Valencia I, Montoya JG. 2015. Right arcuate fasciculus abnormality in chronic fatigue syndrome. *Radiology* **274**:517–526. doi:10.1148/radiol.14141079

Zhang H, Schneider T, Wheeler-Kingshott CA, Alexander DC. 2012. NODDI: Practical in vivo neurite orientation dispersion and density imaging of the human brain. *NeuroImage* **61**:1000–1016. doi:10.1016/j.neuroimage.2012.03.072

Zhang J, Zhong S, Zhou L, Yu Yamei, Tan X, Wu M, Sun P, Zhang W, Li J, Cheng R, Wu Y, Yu Yanmei, Ye X, Luo B. 2021. Correlations between Dual-Pathway White Matter Alterations and Language Impairment in Patients with Aphasia: A Systematic Review and Meta-analysis. *Neuropsychol Rev* **31**:402–418. doi:10.1007/s11065-021-09482-8

> ***Reviewing Editor:***
>
> *I encourage the authors to incorporate the suggestions of the reviewers, such as:*
>
> *(1) to provide more in-depth interpretations about how and why structural and functional lateralization relate,*

Done.

> *(2) to provide statistical effect sizes,*

Done.

> *(3) to make their sulcal-morphology classification openly available,*

Done.

> *(4) to provide statistical effect sizes,*

Done

> *(5) to discuss the possible impact of diverging PT definitions with regard to previous studies,*

Done.

> *(6) to provide more in-depth interpretations about how and why structural and functional lateralization relate.*

Done.

> *Detailed comments:*

> *In an impressive cohort of 907 human participants, the present paper presents a very interesting set of data on PT asymmetries not only at the macro-structural but also at the microstructural levels in order to investigate their potential correlates with PT functional asymmetry in relation to perceptual acoustic language tasks.*
>
> *I believe this is a key paper for the following reasons:*
>
> *(1) it provides critical data and results for addressing a controversial but important question: the relevance of measures of anatomical asymmetry for inferring its language-related functional hemispheric specialization;*
>
> *(2) to do so, the authors made a very impressive effort to manually trace the anatomical delineation of the planum temporale at different levels in every participant, the best (but crazy time-consuming) approach so far to document interindividual variability of the PT and to address such a question;*
>
> *(3) the contribution is particularly relevant regarding the statistical power of the study, the study and measures having been done in 907 participants!*
>
> *(4) I also found the study well designed and well written with great relevance of the findings for the field.*
>
> *As the results, the authors reported asymmetric measures of microstructural asymmetry (including intracortical myelin content, neurite density, and neurite orientation) but also of macrostructural asymmetries in relation to functional lateralization for language.*
>
> *Comments：*
>
> *I have only 2 additional minor comments of my own:*
>
> *(1) In agreement with reviewer 2, I don't understand why the authors seem to downplay the links they found between gross PT asymmetry and functional lateralization. I recommend the authors to highlight and discuss this important result, just as the microstructural PT asymmetries and their functional links.*

This has been done (page 18, line 363-370).

> *(2) PT structural asymmetry (both micro & macro) has been well documented in nonhuman primates (and their functional link with manual lateralization for gestural communication). Without detailing this literature, I recommend the authors at least mention this literature as a comparative perspective in the introduction and/or discussion in order to make the question of PT asymmetry less anthropocentric.*

This has been done (page 15, line 281-288).

https://doi.org/10.7554/eLife.95547.2.sa0